ET_rF vs NDVI Relationships for Southern Idaho for Rapid Estimation of Evapotranspiration

Richard Allen, Clarence W. Robison, Magali Garcia, Ricardo Trezza, M. Tasumi and Jeppe Kjaersgaard

Univ. Idaho, Kimberly, ID

April 2010

Application of the METRIC process to determine ET_rF for irrigated lands is a time consuming process that does not allow for quick estimates of ET in a "real" time mode. In this document, linear relationships between ET_rF and top of atmosphere NDVI are explored with the objective of determining a linear relationship between ET_rF and NDVI that will provide relatively rapid, near-real time estimates of ET_rF to be made using LandSat or other satellite imagery. ET_rF represents the 'fraction' of reference ET and is synonymous with the widely known crop coefficient (K_c). In practice, ET for a pixel is calculated as $ET = ET_rF \times ET_r$ where ET_r is reference ET computed for an alfalfa reference crop using, preferably, the ASCE-EWRI Standardized Penman-Monteith equation (ASCE-EWRI 2005). In some situations ET_r from Agrimet, which is computed using the 1982 Kimberly Penman equation, can be substituted. The NDVI-based procedure is efficient, time-wise, and can be applied with Landsat, SPOT, AWIFS or even with the MODIS 16-day vegetation index products where effects of clouds have largely been removed. It is essential, however, that the ET_rF vs VI relationships first be calibrated using the METRIC surface energy balance model, so that the simplified relationships accurately account for effects of evaporation from soil.

Background on the Application of METRIC

Briefly, METRIC is an energy balance process that determines actual ET and then ET_rF as a residual of the energy balance (Allen et al. 2007) ($ET = R_n - G - H$) where R_n is net radiation, G is soil heat flux density and H is sensible heat flux density convected to the air. In application of the METRIC process to remotely sensed imagery; the sensible heat (H) is calibrated for each image date using a "cold" and a "hot" pixel located in the vicinity of a nearby reference weather station. The quality review of the meteorological data from the weather station and the actual selection of the hot and cold pixels can be time intensive. After a selection of a hot and cold pixel pair, the resulting ET_rF image is reviewed and the calibration process repeated. As generally applied, the METRIC process produces ET_rF for each image date, rather than actual ET, so that ET_rF can be interpolated between satellite dates using a cubic spline to produce daily images of ET_rF. These daily ET_rF images are then multiplied by ET_r to produce daily ET.

The METRIC ET_rF is a surrogate for crop coefficient K_c and represents the reference evapotranspiration fraction occurring from a land surface. This includes both the evaporation from the soil surface and transpiration from vegetation. The complete formulation for K_c (Allen et al. 1998) is:

[1]

or in terms of ET_rF

[2]

where:

K_{cb} is the basal crop coefficient of the vegetation that is most directly related to NDVI

K_e is the soil evaporation coefficient that is dependent on the amount of moisture remaining in the surface layer of the soil and on the amount of vegetation covering (shading) the soil surface (Allen et al., 1998, 2005b,c).

During full vegetation cover (i.e., high NDVI), K_e will typically be less than 0.1, even for a wet soil surface). For bare surfaces, K_e is limited by the amount of moisture in the upper soil surface, typically the upper inch and depends on the soil type and values can range from 0 to 1.0 as shown in Figure 1. The soil evaporation component of ET can range from 20 to as high as 35%, under southern Idaho conditions. The range of the evaporation component depends on wetting frequency.

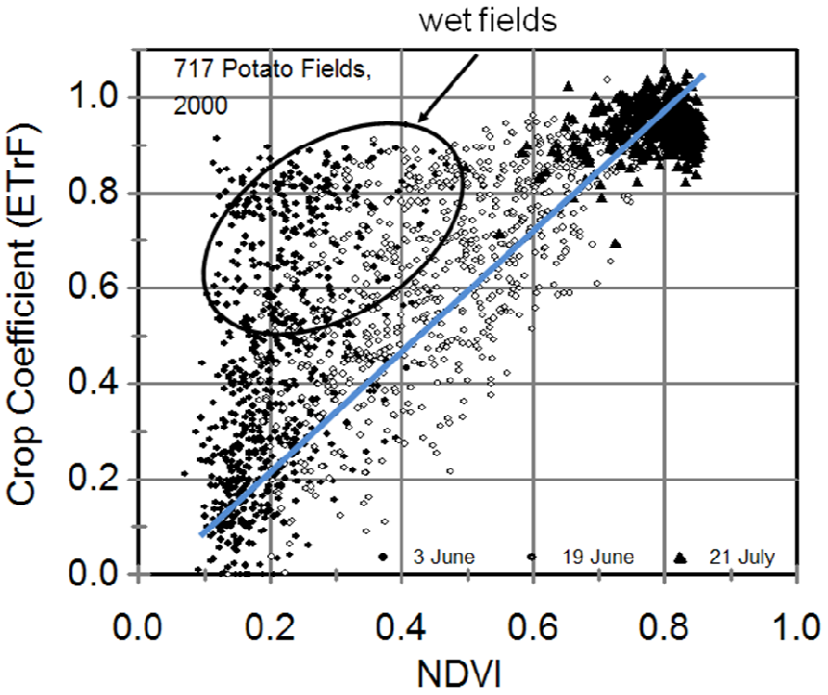

Figure 1. Crop coefficients (ET_rF) derived from METRIC energy balance based applications with Landsat for potatoes in Magic Valley of southern Idaho for year 2000 showing the deviation of ET_rF from a universal, linear transpiration line when fields are wet. Each point represents one field on one satellite date. ET_rF is "fraction of reference ET" and is synonymous with K_c.

Studies by Tasumi and Allen (2007) and Allen et al. (2010, manuscript in final preparation) indicate that universal, linear equations relating actual ET_rF to VI may be applicable for regional estimates when calibrated using energy balance-derived ET. Their testing of the calibrated ET_rF vs. VI approach demonstrated that ET can be estimated without conducting a crop type

classification, which can be costly. The calibrated ET_rF values include effects of evaporation from soil.

The idea of correlating ET and VI's is not new, having been explored some years ago by Bausch and Neale, 1989, Neale et al., (1989) and Choudhury et al., (1994). Generally, VI's are calculated as ratios or normalized differences between two spectral bands (Payero et al., 2004). Examples of VI's are the NDVI and SAVI. Because VI's do not accurately capture specific soil evaporation or reduced ET caused by acute water shortage, this approach is generally most accurate for estimating "basal" K_c (K_{cb}) rather than "actual" K_c (Neale et al., 2005), where K_{cb} is defined as the K_c for a vegetated surface having dry soil surface but with adequate soil water content in the root zone to support full ET (Wright, 1982, Allen et al., 1998). Recent studies indicate that K_c and K_{cb} tend to be linear to NDVI (Allen et al., 2005; Hunsaker, 2003; Duchemin et al., 2006, Allen et al. 2010). K_{cb} is proportional to VI because K_{cb} represents primarily the transpirative component of ET (i.e., $K_{cb} \sim T/ET_r$), and T is generally proportional to the amount of vegetation present. As shown in the following text, however, the soil evaporation component, when averaged over a large number of fields and extended time period, can be 'blended' into an ET_rF vs. NDVI with good results. Therefore, ET_rF vs NDVI can be expressed two ways. In the combination VI plus soil evaporation method, actual ET is estimated as:

$$\begin{aligned} ET_rF &= K_{cb} + K_e \\ K_{cb} &= a + b(VI) \text{ and } K_e = f(\textit{wetting frequency}) \\ ET &= ET_rF \times ET_r \end{aligned} \qquad [3]$$

In regions where precipitation amounts and frequency are consistent from year to year, and where ET estimates are needed over large numbers of fields, rather than for specific fields, one can avoid direct estimation of K_e by blending K_e into the ET_rF relationship:

$$\begin{aligned} ET_rF &= a + b(VI) \\ ET &= ET_rF \times ET_r \end{aligned} \qquad [4]$$

It is Eq. 4 that is proposed for rapid application by IDWR. I is recognized that any evaporation from exposed soil following rain or irrigation events will add to the total ET amount, but is not be reflected in the VI. Therefore, these 'averaged' effects of evaporation are incorporated into the ET_rF vs. VI relationship. For example, Figure 1 shows the correspondence between ET_rF derived from the METRIC energy balance for about 700 potato fields in southern Idaho, where the solid blue line represents the general K_{cb}, or transpirative component of ET. The large numbers of points (fields) extending above the blue line represent fields that were wet from irrigation at the time of the satellite image. It is important to include that component of water depletion in the ET estimate.

NDVI, SAVI and EVI

Normalized Difference Vegetation Index, NDVI, and the Soil Adjusted Vegetation Index (SAVI: Huete, 1988) are popular vegetation indices because they require only two spectral bands (red and near infrared) and the normalization provided by the denominators typically adjusts for some atmospheric variation, sensor calibration, and soil background. NDVI is calculated as:

$$NDVI = \frac{ref_{NIR} - ref_R}{ref_{NIR} + ref_R} \quad [5]$$

where ref_R and ref_{NIR} are at-satellite or at-surface reflectances in the red and near infrared satellite bands (Landsat bands 3 and 4 or MODIS bands 1 and 2). At-satellite NDVI, denoted as $NDVI_{sat}$, is based on satellite-derived reflectances, but without atmospheric correction. Alternatively, NDVI can be computed using surface reflectance values that have been atmospherically corrected. This NDVI, referred to as at-surface NDVI, i.e., $NDVI_{surf}$ can produce a more consistent value for NDVI from image to image as atmospheric conditions change. However, as shown in this report, the improvement in the ET_rF vs. NDVI is small. In general agricultural settings, the value range of $NDVI_{sat}$ is roughly 0.1 - 0.15 for bare soil) to 0.80 - 0.85 for full vegetation cover, whereas the range of $NDVI_{surf}$ is roughly about 0.1 - 0.15 and 0.85 - 0.95.

SAVI is calculated similar to NDVI as:

$$SAVI = \frac{ref_{NIR} - ref_R}{ref_{NIR} + ref_R + L}(1 + L) \quad [6]$$

where L is a constant that reduces the impact of the soil background reflectance and wetness. Values for L range from 0 to 1, with the value L = 0.5 used in most applications (Huete, 1988). METRIC applications in Idaho have used L = 0.1 based on calibrations in Magic Valley (Allen et al., 2007a). Under low vegetation conditions, SAVI is expected to estimate vegetation vigor more consistently than NDVI by reducing the impact of background soil surface (Huete, 1988). Under dense vegetation conditions, SAVI is considered to be more tolerant to "saturation" of the VI computation than NDVI (Payero et al., 2004). However, this may not be an advantage over NDVI, as shown in a following comparison.

Besides NDVI and SAVI, several "advanced" vegetation indices (VIs) have been suggested, including the Transformed Soil Adjusted Vegetation Index (TSAVI: Baret and Guyot, 1991), and the Enhanced Vegetation Index (EVI: Huete et al., 1997). The EVI is a commonly derived VI for MODIS imagery and uses reflectance from the 'blue' band of images in addition to the red and near-infrared bands. However, these VI's are not applied here because of the consistency found for the NDVI relationships.

When correcting reflectances for atmospheric attenuation, the amount of correction varies with satellite band. Often, relatively sophisticated radiation transfer models (RTM's) are used for atmospheric correction, for example, MODTRAN and S6 (Berk et al., 2002, Vermote et al., 2002). These models generally require atmospheric profiles of water vapor and temperature from radiosondes and assumptions regarding amount and composition of aerosols. Tasumi et al., (2008) developed a simplified atmospheric model, calibrated using MODTRAN-derived correction, that only requires an external estimate of atmospheric water content, and does not

require the use of radiosondes. Accuracy of this method is relatively high in clean air conditions expected over agricultural areas and agrees closely with atmospheric corrections made by the MODIS products that are profile based (Tasumi et al., 2008). The Tasumi method can be utilized to derive relatively rapid, surface-level $NDVI_{surf}$, however, if the Department wishes to utilize $NDVI_{surf}$ rather than $NDVI_{sat}$. An estimate of near surface vapor pressure is required.

Derivation of ET_rF vs.Vegetation Indices for Southern Idaho

ET_rF vs.Vegetation Index relationships were derived for two years of data for southern Idaho. These two years were year 2000 and year 2006. Data for these two years were based on intensive application of the METRIC energy balance process. The development of ET_rF vs. VI relationships was done independently for 2000 and for 2006. Development of the relationships for year 2000 is discussed first.

METRIC ET_rF was determined for 12 Landsat images in year 2000 for path 40, row 30 that overlays Magic Valley. The images had a 16 to 32 day frequency. A crop-type classification was conducted using the Landsat images and independent ground truth information. Following the classification, a total of 3420 fields from the area outlined in Figure 2 were sampled that included eight crop types (Table 1). The field samples were taken from locations about 40% in from field edges to eliminate effects of contamination of thermal or short wave information by areas outside the fields. Landsat image georegistration error was generally less than 15 m. Figure 3 shows K_c data sampled for the winter grain crop as presented from a previous study (Tasumi et al, 2005) where K_{cr} represents the actual (mean) K_c (i.e,. ET_rF) based on an alfalfa reference ET (ASCE, 2005). A single pixel sample was used to sample ET and K_c from each field, based on relatively uniform fields. Later comparisons with multiple sampled pixels per field indicated that error in K_c averaged over large numbers of fields was statistically zero when the number of fields in the average exceeded 50.

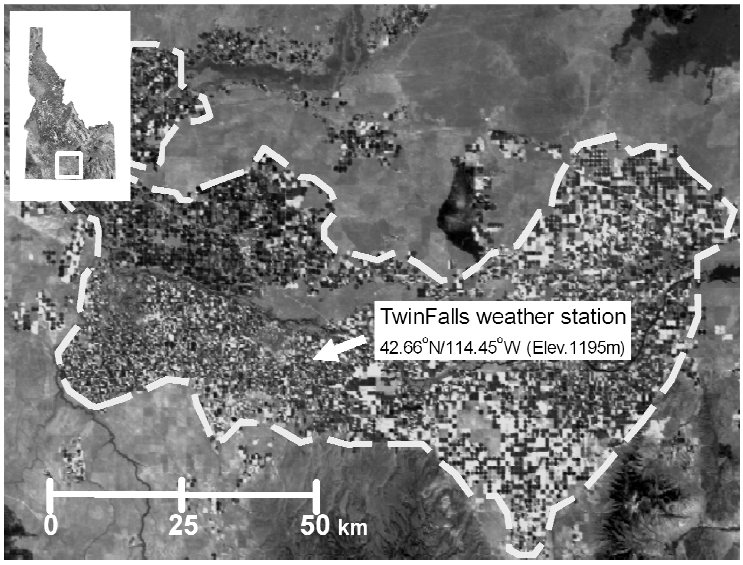

Figure 2. Agricultural study area in Magic Valley, Idaho (outlined by the dotted line) and location of the weather station used to calculate reference ET in the surface energy balance and in derivation of crop coefficients (ET_rF).

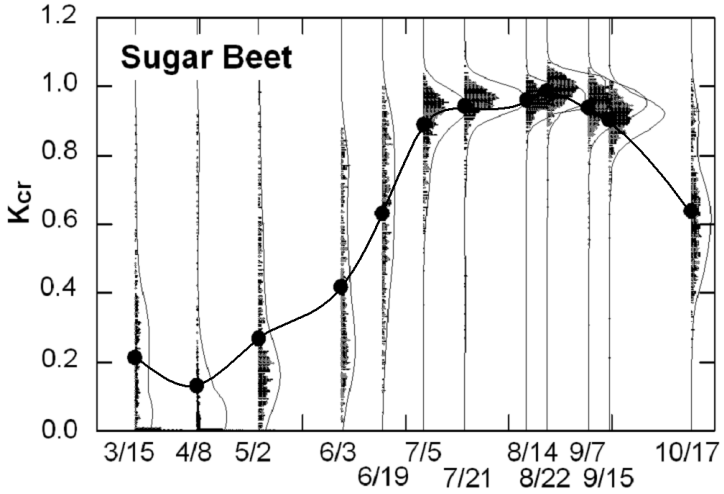

Figure 3. Alfalfa-reference based K_c for 564 sugar beet fields in Magic Valley, Idaho during 2000 plotted for each satellite date (vertical lines). Curved, fine lines represent general shapes of the probability density functions.

Table 1. Investigated crops and numbers of sampled fields for year 2000.

Crop type	Alfalfa	Bean	Corn	Potato(S)*	Potato(L)*	Sugar Beet	Spring Grain	Winter Grain	Total
Sample field	325	432	451	396	221	495	536	564	3420

* Potato(S) and Potato(L) are potato crops having short (S) and long (L) full cover periods respectively.

Data from all fields containing the same crop type were averaged into a simple ET_rF vs. VI pair for each Landsat date. The vegetation indices evaluated were $NDVI_{sat}$, $NDVI_{surf}$, $SAVI_{sat}$ and $SAVI_{surf}$. ET_rF was expressed on the basis of alfalfa reference ET (expressed in some of the following figures as K_{cmr} or K_{cr}).

Figure 4 shows ET_rF vs VI relationships obtained for all crops in the study area for both at-surface (s) and at-satellite (as) NDVI and SAVI. METRIC ET from Tasumi et al. (2005) was used to represent actual ET. Relationships between ET_rF and VI in Figure 4 represent only periods during crop development stages (as opposed to late season periods), as ET_rF relationships were more variable among crops during periods of crop senescence. As illustrated in Figure 4, crops had similar ET_rF vs. NDVI or ET_rF vs. SAVI trends during development periods. Because the ET_rF vs NDVI and SAVI relationships among the investigated crops were similar, an overall, generalized equation was developed, common to all crops as:

$$ET_rF = a + b\ VI \qquad [7]$$

where a and b are slope and intercept determined through calibration. This generalized equation can be applied without the need for crop classification, which is a valuable asset, as crop classification is typically a time consuming and expensive process. Alfalfa hay crops were not included in the determination of the general ET_rF vs. VI functions because of the random, irregular cutting

schedules among individual alfalfa fields. However, the relationships derived for the other crops fit alfalfa relatively well, as shown later.

Results and Discussion for year 2000

The spring period of year 2000 was relatively dry, precipitation wise, in constrast to 2006, where March-April precipitation in 2000 was only 38% of 2006 and 56% of average and April-May precipitation in 2000 was only 50% of 2006 and 64% of average (2006 had a relatively wet spring at 150% and 132% of average for March-April and April-May). Monthly precipitation recorded at the Kimberly Agrimet weather station (TWFI) is summarized in Table 2.

Table 2. Monthly and annual precipitation and reference ET for the Twin Falls Agrimet weather site near Kimberly for years 2000 and 2006 plus an 18 year average. The reference ET is based on the ASCE-EWRI Penman-Monteith equation.

Year	Jan.	Feb.	**Mar.**	**Apr.**	May	June	July	Aug.	Sep.	Oct.	Nov.	Dec.	Ann.
Precipitation, mm													
2000	42	37	**17**	**14**	29	2	0	2	13	33	11	19	218
2006	48	17	31	51	36	19	8	0	4	21	32	50	317
1991-2008	29	18	24	31	35	20	7	10	11	18	24	35	260
Reference Evapotranspiration, mm													
2000	34	53	109	174	199	274	267	230	173	114	37	25	1690
2006	34	50	83	131	208	239	254	235	167	99	54	32	1586
1991-2008	35	49	104	137	188	221	253	226	167	114	54	33	1580

As a consequence of year 2000 being drier than average and 2006 being wetter than average, derived ET_rF relationships are expected to deviate between the two years.

The advantage of developing calibration coefficients based on averaged ET_rF and VI's as plotted in Figure4 is that the regression equation determined from fitting to the data is not impacted as much during the least-squares fitting as it would be if ET_rF from individual fields were regressed, where outlying (i.e., high values for) ET_rF tend to bias the least-squares regression toward those points. This somewhat with regressions derived from 2006 data where individual field data were regressed (discussed later).

Calibration coefficients for year 2000 for Eq. 7 are summarized in Table 3. Comparison of the fit of data in Figure 4 for NDVI and Figure 5 for SAVI and statistics in Table 3 indicate that both at-surface reflectance (corrected for atmospheric attenuation) and at-satellite (non corrected)) indices and both NDVI and SAVI all provide similar fits and linearity between ET_rF and VI's for most crops. Even though the at-surface VI's utilize true (at-surface) reflectances, as compared to reflectances computed at satellite, the VI's are not substantially altered by the atmospheric correction. The lack of impact is primarily because atmospheric attenuation in bands 3 and 4 of Landsat are of similar magnitude and because reflectances show up in both the numerator and denominator of the NDVI and SAVI functions. The small impact of atmospheric correction in the VI's indicates that atmospheric effects among the six Landsat images sampled in constructing Figures 4 and 5 were similar.

In figures 4 and 5, winter grain (wheat and barley) exhibited a reduction in ET_rF with increasing VI between about 0.2 and 0.4 (for NDVI) and 0.3 (for SAVI). This behavior was caused by relatively wet soil conditions early in the growing season when ET_rF and VI were first sampled for winter grains, but relatively dry conditions during the second sampling (i.e., second image in April). This second sampling period was still prior to the beginning of the irrigation season and it is possible that some of the winter grain fields were subjected to moisture stress. Similar behavior (higher ET_rF at lower VI during the first date sampled than during the second date sampled) was exhibited by spring grain and dry beans, but the range in VI was smaller than for winter grain.

ET_rF vs. VI pairs for potatoes, sugar beets and corn tended to plot above the plots for the other crops and above the mean relationship established for all crops combined. The general relationships (solid lines) established in Figures 4 and 5 are useful for estimating ET_rF from VI in the absence of knowledge of specific crop type. General adherence of ET_rF vs. VI relationships by the six crops to a general curve reflect the close relationship between transpiration and vegetation amount as reflected in the VI. Also, the close correspondence among crops suggests similar amounts of evaporation resulting from precipitation and irrigation. Potatoes are generally irrigated more frequently than other crops and thus are expected to have higher ET_rF for the same VI. However, many of the fields sampled were irrigated by center pivot so that even corn and sugar beets probably had frequent wetting, in general.
One interesting phenomenon with ET_rF – SAVI pairs was the tendency for values for SAVI to display a broad range near the highest levels of ET_rF (Figure 5). This range in SAVI occurs because of a tendency for ET_rF to approach a maximum value (near 1.0) when vegetation cover is near, but perhaps 5 to 10% less than complete full cover. NDVI at this high end of vegetation cover tends to saturate at about the same point where ET_rF reaches a maximum. Therefore, a linear relationship between ET_rF and NDVI tends to occur. In the case of SAVI, SAVI's lower tolerance to "saturation" in dense vegetation conditions appears to be a disadvantage when estimating ET_rF and it causes a sort of 'plateau' in ET_rF at high values for SAVI. Because of the phenomenon, the NDVI is preferred for application.

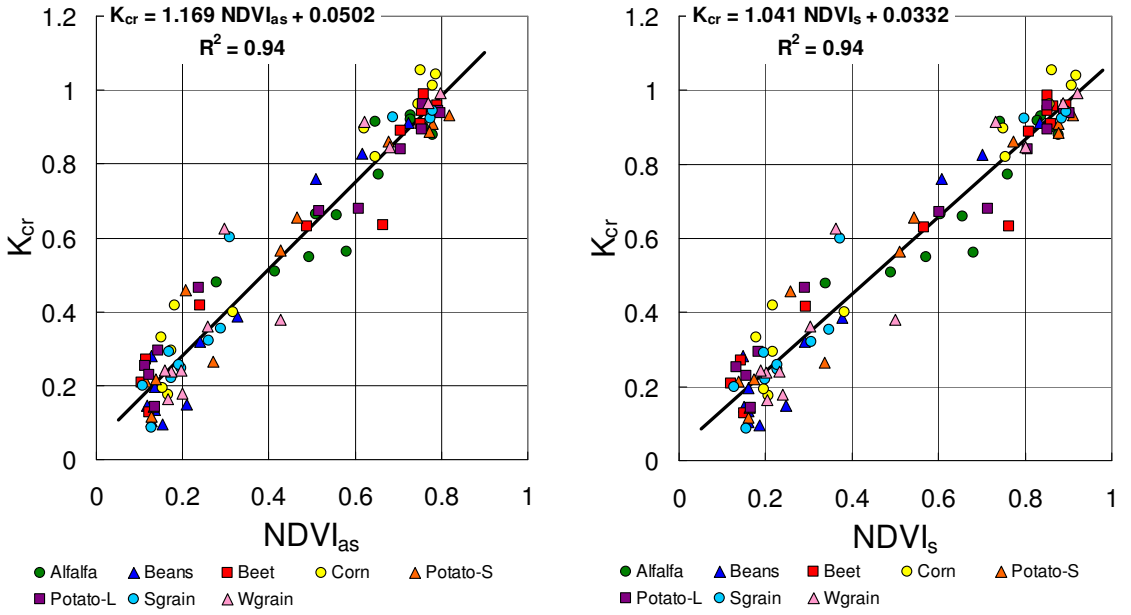

Figure 4. ET_rF vs. $NDVI_{sat}$ and $NDVI_{surf}$ by crop type during crop development stages for year 2000 field averages by crop.

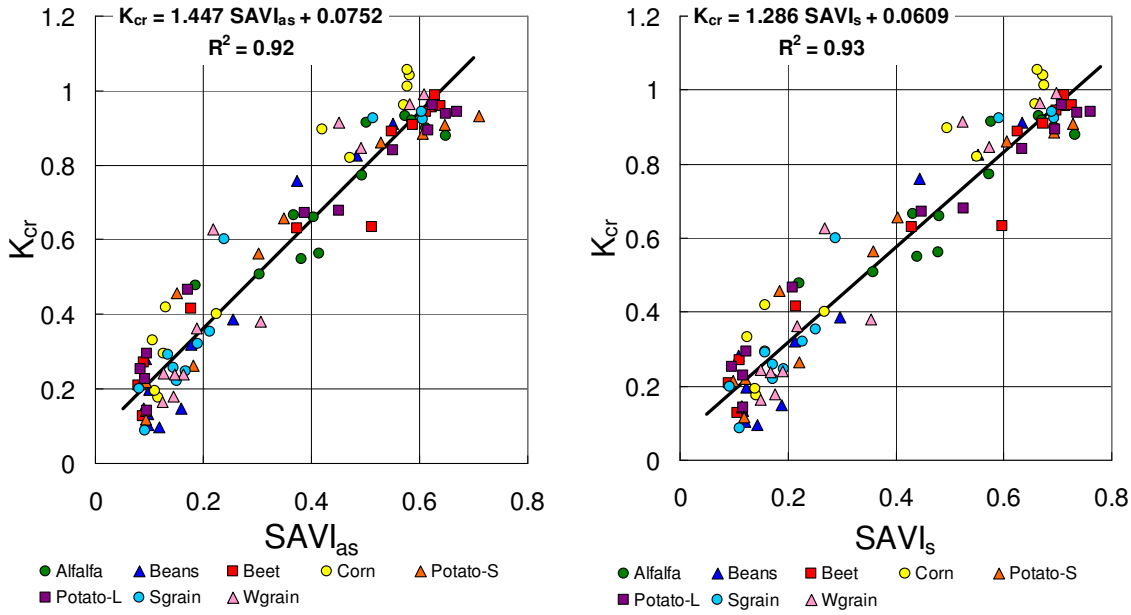

Figure 5. ET_rF vs. $SAVII_{sat}$ and $SAVI_{surf}$ by crop type during crop development stages for year 2000 field averages by crop.

Table 3. Calibrated slopes and intercepts for Equation 7.

Constants	NDVIsat	NDVIsurf	SAVIsat	SAVIsurf
slope	1.169	1.041	1.447	1.286
intercept	0.0502	0.0332	0.0752	0.0609
R^2	0.94	0.94	0.92	0.93

Recommended ET_rF vs. NDVI relationship

Because the at satellite $NDVI_{sat}$ (also known at the 'top of atmosphere' NDVI) performed as well as the atmospherically corrected $NDVI_{surf}$ parameter, we recommend that $NDVI_{sat}$ be used to estimate ET_rF for convenience. The resulting equation from Year 2000 data was:

$$ET_rF_{2000} = 0.05 + 1.17\, NDVI_{sat} \quad [7a]$$

However, as shown later, in year 2006, spring conditions were wetter and therefore values for ET_rF were about 15% higher under conditions of bare soil. Therefore, the offset in Eq. 7 was higher. As discussed later, a general equation derived from 2006 data had the form:

$$ET_rF_{2006} = 0.23 + 0.90\, NDVI_{sat} \quad [7b]$$

Eq. 7a estimates $ET_rF = 0.2$ at NDVI = 0.12 (bare soil) and $ET_rF = 1.0$ at NDVI = 0.8 (dense cover), whereas Eq. 7b estimates $ET_rF = 0.34$ at NDVI = 0.12 (bare soil) and $ET_rF = 0.95$ at NDVI = 0.8 (dense cover). The higher ET_rF at low NDVI in 2006 was due to the wetter spring. The lower ET_rF at high NDVI in 2006 was probably due to influences of potatoes (discussed later) that may have exhibited $ET_rF < 1.0$ even at high NDVI (full cover). This phenomenon is somewhat apparent for potatoes in 2000 also (see Fig. 5), although not to a large extent.

Because the spring of 2000 was drier than average and the spring of 2006 was wetter than average (Table 2), the lower ends of Eq. 7a and 7b were combined to better represent an average rainfall condition. This was done by adding 8% (approximately half the difference between 2000 and 2006 ET_rF for low NDVI conditions) to the lower end of the relationship and then developing a new equation. The value for ET_rF at NDVI = 0.8 was retained at 1.0, following 2000, however, to be consistent with average observed ET_rF values by Wright (1982) in the Kimberly lysimeters and based on general outcomes with METRIC applications in southern Idaho. The resulting generalized equation is therefore:

$$ET_rF = 0.15 + 1.06\ NDVI_{sat} \quad [8]$$

where Eq. 8 is recommended for application in near-real time. Eq. 8 estimates $ET_rF = 0.28$ at NDVI = 0.12 (bare soil) and $ET_rF = 1.0$ at NDVI = 0.8 (dense cover).

Tests of accuracy

Allen et al. (2010) tested the accuracy of seasonal ET estimated using Equation 4, with ET_rF estimated from Eq. 7a ($ET_rF_{2000} = 0.05 + 1.17\, NDVI_{sat}$)and where daily ET_rF, following its estimation from NDVI, was splined between satellite images and multiplied by daily reference

ET calculated from weather data. The performance accuracy of ET based on VI was evaluated by comparing against METRIC ET, which was based on a complete energy balance.

As shown in Table 4 and Figure 6, ET derived from NDVI, where the ET_rF was calibrated using the METRIC energy balance, and where only a general K_c vs. NDVI relationship was used (crop classification free), estimated ET with affordable accuracy for the primary crops grown in southcentral Idaho. The seasonal error was within 7 % for all crops except beans. The relatively high accuracy in estimating average seasonal ET over a large area using a single linear equation is important finding, because it implies that the suggested technique may often not require crop-type classification to estimate ET. Estimates by Eq. 8 using average 2000 + 2006 precipitation conditions, are expected to be similar.

Allen et al. (2010) also noted that even though NDVI is a more simple index than SAVI, it produced better estimates of ET. A primary advantage of SAVI is to reduce the impact of background soil bias under low vegetation conditions. However SAVI based ET increased error in ET_rF estimation for dense vegetation because of SAVI's tendency to extend the point of signal 'saturation' to relatively high vegetation densities. The 'saturation' of the NDVI signal for dense vegetation conditions happens to occur at about the same point where ET_rF tends to saturate (i.e., maximize). This is strong advantage when estimating ET.

Table 4. Error (%) in seasonal ET estimated using NDVI and SAVI vegetation indices relative to seasonal ET calculated by METRIC – positive values indicate overestimation.

Crops	METRIC ET (mm)	NDVIsat	SAVIsat
Alfalfa	1001	5.0	3.8
Beans	479	8.5	9.5
Beet	904	-1.7	-0.2
Corn	846	-6.3	-10.7
Potato-S	733	2.0	4.8
Potato-L	846	-1.5	0.5
S.Grain	720	-0.9	-0.3
W.Grain	837	-1.4	-4.2
Ave. Abs. Error	-	4.6	6.1

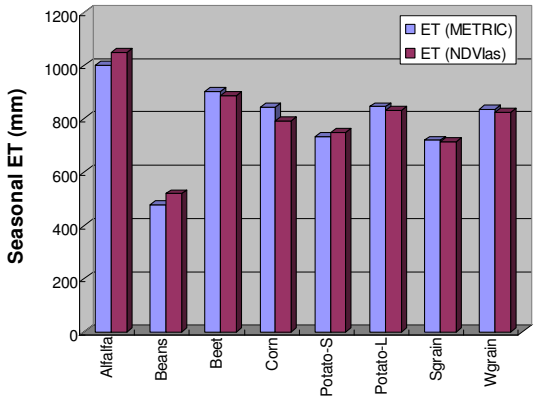

Figure 6. VI based seasonal ET estimates compared with METRIC ET using NDVI.

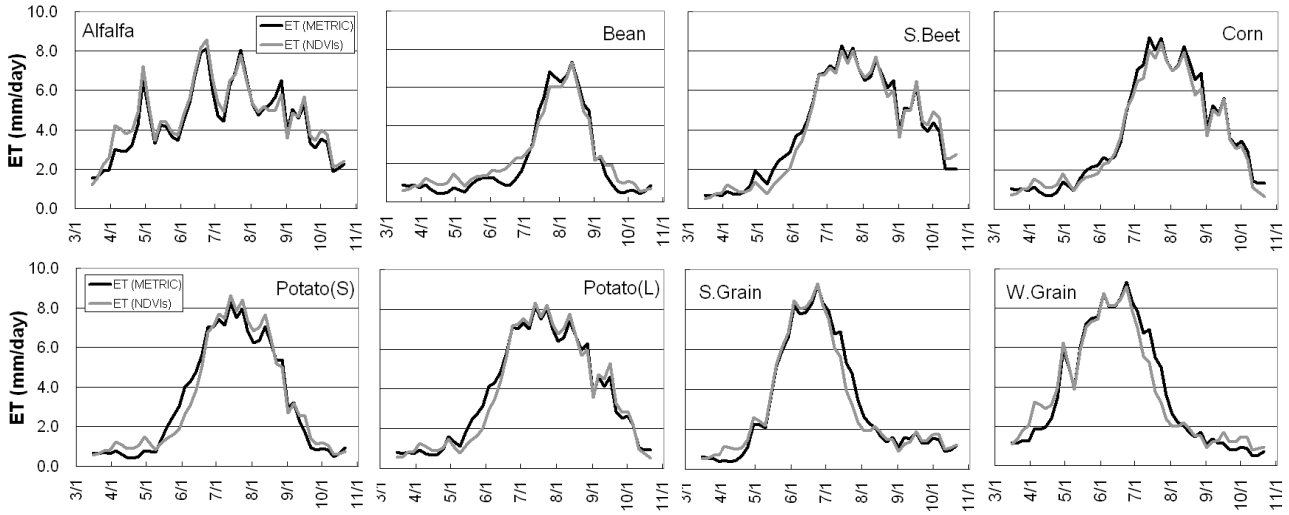

Figure 7. Comparisons between 5-day ET determined by METRIC for specific crops and ET determined from the general $ET_rF_{2000} = 0.05 + 1.17\, NDVI_{sat}$ relationship, averaged over hundreds of sampled fields in southern Idaho.

Comparisons with ET measured by lysimeter

Allen et al., (2010) tested performance accuracy of VI based ET estimation at two fields equipped with precision weighing lysimeters near Kimberly, Idaho. The lysimeter ET data were collected by Dr. J.L.Wright at the USDA Agricultural Research Service facility during the 1970's and 1980's (Wright, 1982 and 1991). NDVI computed for satellite image dates was interpolated for days between dates using a cubic spline function and ET_rF was estimated using Equation 7a. Daily ET was estimated using Equation 4 by multiplying by daily ET_r. Comparisons of estimated to measured ET are shown in Figure 8 on a daily basis and in Figure 9 on a seasonal basis. The VI based ET estimations corresponded relatively well with the actual lysimeter measurements, for both the grass and sugar beet fields. The standard error of daily ET estimates as compared to lysimeter measurements was 0.6 mm d^{-1} and 1.3 mm d^{-1}, respectively for grass and sugar beets. As made obvious in the daily comparison for the sugar beets, the VI based method, where the evaporation coefficient, K_e, is not explicity calculated, was unable to capture increased evaporation caused by irrigation events. These events are manifested as spikes in ET in Figure 8. On a seasonal basis, the NDVI-based ET estimated estimated seasonal ET within 2% for grass and 6% for sugar beets as measured by the two lysimeter fields during 1989, even though the NDVI calibrations were made using data from year 2000. Estimates by Eq. 8 using average 2000 + 2006 precipitation conditions, are expected to be similar.

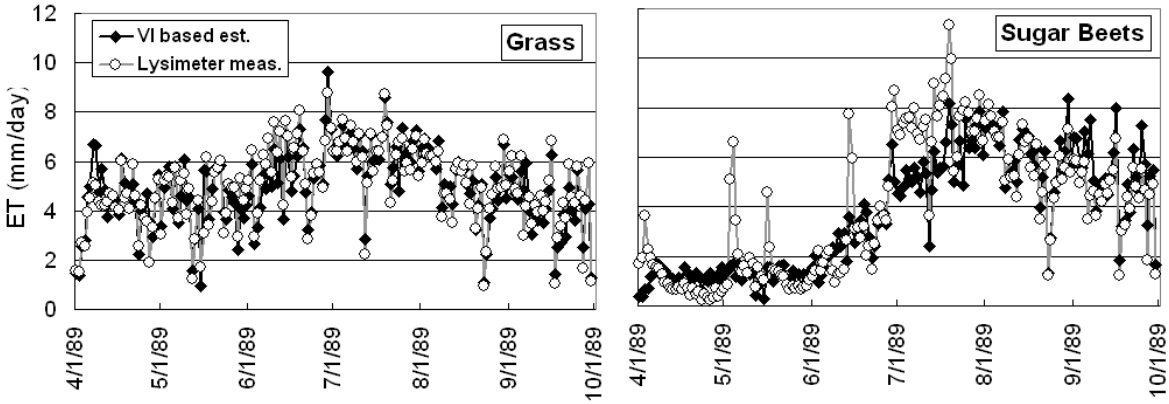

Figure 8. Comparisons of estimated daily ET based on NDVI with ET measured by lysimeter for two fields (grass-left and sugar beets-right).

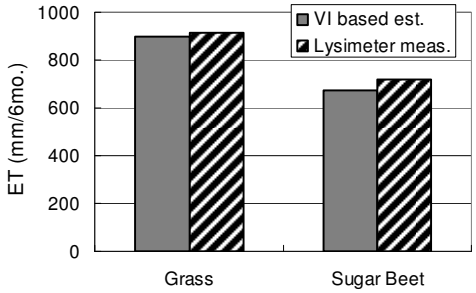

Figure 9. Comparison of seasonal ET estimated from METRIC calibrated NDVI based ET_rF and lysimeter-based measurements during 1989 at Kimberly, Idaho (April to September periods).

The analysis of year 2006 is described in Appendix A.

Application Procedure

The recommended procedure for applying the ET_rF vs. NDVI procedure in near real-time is as follows:

a. Obtain Landsat or other satellite images
b. Calculate top-of-atmosphere (at-satellite) reflectances for the red and near infrared bands (bands 3 and 4 in Landsat)
c. Calculate $NDVI_{sat}$ from Eq. 5.

d. Repeat steps a-c for a second image (in time).

e. use a spline or other interpolation function to calculate NDVI images for every day between the two image dates. An ERDAS Spline model, set up for splining NDVI, has been created by the UI and is available at: http://www.kimberly.uidaho.edu/~rallen/IDWR_NDVI/ for various months of the year. These models will need to be modified for new image dates, however. Also, any clouds will need to be masked out and filled in using some sort of proportioning strategy.
f. Once the daily NDVI images have been created, Eq. 8 is applied to create daily images of ET_rF.
g. The daily images of ET_rF are then multiplied by the reference ET_r from a local station, where the ET_r is preferably based on the ASCE-EWRI Standardized Penman-Monteith equation for the alfalfa reference. The REF-ET software of the Univ. Idaho can be used for this purpose. The weather data should be QA/QC'd for accuracy. If a large area is covered, an ET_r "surface" can be created by kriging, etc. among a series of weather stations.
h. The resulting ET images from step g can then be aggregated in time to produce an image of ET over some time period. These images will reflect the impact of weather on ET (implied in the ET_r calculations) and impacts of vegetation amounts (implied in the NDVI signals). These ET images can be aggregated in space to estimate total ET within a particular water service area.

References

Allen, R. G., Pereira, L. S., Raes, D., and Smith, M. (1998). "Crop evapotranspiration." FAO Irrigation and Drainage Paper 56, Food and Agricultural Organization of the United Nations, Rome.

Allen, R. G., Morse, A., Tasumi, M., Trezza, R., Bastiaanssen, W. G.M., Wright, J. L., and Kramber, W. (2002). "Evapotranspiration from a satellite-based surface energy balance for the Snake River Plain Aquifer in Idaho." *Proc., USCID/EWRI Conf. on Energy, Climate, Environment and Water,* San Luis Obispo, Calif.

Allen, R. G., Tasumi, M., Morse, A., and Trezza, R. (2005a). "A Landsat-based Energy Balance and Evapotranspiration Model in Western US Water Rights Regulation and Planning". *Irrigation and Drainage Systems*. 19:251-268.

Allen, R.G., Pereira, L.S., Smith , M., Raes, D. and Wright, J.L. (2005b). FAO-56 dual crop coefficient method for estimating evaporation from soil and application extensions. J. Irrig. and Drain. Engrg., ASCE 131(1):2-13.

Allen, R.G., Pruitt, W.O., Raes, D., Smith, M. and Pereira, L.S. (2005c). "Estimating evaporation from bare soil and the crop coefficient for the initial period using common soils information." J. Irrig. and Drain. Engrg., ASCE 131(1):14-23.

Allen, R.G., M. Tasumi and R. Trezza. (2007a). "Satellite-based energy balance for mapping evapotranspiration with internalized calibration (METRIC) – Model." *ASCE J. Irrigation and Drainage Engineering* 133(4):380-394.

Allen, R.G., M. Tasumi, A.T. Morse, R. Trezza, W. Kramber, I. Lorite and C.W. Robison. (2007b). "Satellite-based energy balance for mapping evapotranspiration with internalized calibration (METRIC) – Applications." *ASCE J. Irrigation and Drainage Engineering.*

Allen, R.G., M. Tasumi, R. Trezza, J.L. Wright, I. Lorite-Torres, C.W. Robison, T. Morse. (2010). Satellite-based ET mapping for agricultural water management: Estimating Evapotranspiration from vegetation indices. manuscript in final stages of preparation.

Anderson, M., Norman, J., Diak, G., Kustas, W., and Mecikalski, J. (1997). "A two-source time-integrated model for estimating surface fluxes from thermal infrared satellite observations". *Remote Sensing of Environment*, 60, 195–216.

Baret, F., and Guyot, G. 1991. Potentials and limits of vegetation indices for LAI and APAR assessment. *Remote Sensing of Environment.* 35: 161-173.

Bastiaanssen, W. G. M., Menenti, M., Feddes, R. A., and Holtslag, A. A. M. (1998). "A remote sensing surface energy balance algorithm for land (SEBAL): 1. Formulation." *J. Hydrol.*, 212–213, 198–212.

Bastiaanseen,W.G.M. (2000). "SEBAL-based sensible and latent heat fluxes in the irrigated Gediz Basin, Turkey". *J. of Hydr*. 229:87-100.

Bastiaanssen, W. G. M. and Ali, S. (2003). "A new crop yield forecasting model based on satellite measurements applied across the Indus Basin, Pakistan". *Agriculture, Ecosystems and Environment* 94 (2003) 321–340

Bausch, W. C., and Neale, C. M. U. (1989). "Spectral Inputs Improve Corn Crop Coefficients and Irrigation Scheduling." *Transactions of the ASAE*, 32(6):1901-1908.

Berk, A., G.P. Anderson, P.K.Acharya, L.S. Bernstein, et al. 2002. MODTRAN5: A reformulated atmospheric band model with auxiliary species and practical multiple scattering options. Proceedings, NASA/AVIRIS Workshop, Reston, VA.

Burt, C.M., Mutziger, A.J., Howes, D.J., and Solomon, K.H. (2005). "*Evaporation from irrigated agricultural land in California*." Study funded by CAFED and Calif. Tate Univ./Agric. Initiative. (http://www.itrc.org/reports/reportsindex.html)

Choudhury, B. J., Ahmed, N. U., Idso, S. B., Reginato, R. J., and Daughtry, C. S. T. (1994). "Relations between evaporation coefficients and vegetation indices studies by model simulations." *Remote Sens. Environ*., 50, 1–17.

Duchemin, B., Hadria, R., Erraki, S., Boulet, G., Maisongrande, P., Chehbouni, A., Escadafal, R.,

Ezzahar, J., Hoedjes, J. C. B., Kharrou, M. H., Khabba, S., Mougenot, B., Olioso, A., Rodriguez, J.-C., and Simonneaux, V. (2006). "Monitoring wheat phenology and irrigation in Central Morocco: On the use of relationships between evapotranspiration, crops coefficients, leaf area index and remotely-sensed vegetation indices". *Agricultural Water Management* 79(1):1-27.

EWRI. (2005). "The ASCE standardized reference evapotranspiration equation." Environmental and Water Resources Institute of the ASCE Standardization of Reference Evapotranspiration Task Committee (EWRI).

French, A. N., Jacob, F., Anderson, M. C., Kustas, W. P., Timmermans, W., Gieske A., Su, Z., Su, H., McCabe, M. F., Li, F., Prueger, J., and Brunsell, N. (2005). "Surface energy fluxes with the Advanced Spaceborne Thermal Emission and Reflection radiometer (ASTER) at the Iowa 2002 SMACEX site (USA)" *Remote Sensing of Environment*. 99(1-2):55-65.

Howell, T.A., Evett, S.R., Tolk, J.A. and Schneider, A.D. (2004). Evapotranspiration of Full-, Deficit-Irrigated, and Dryland Cotton on the Northern Texas High Plains. *J. Irrig. and Drain. Engrg.*, ASCE 130(4):277-285.

Garcia, Magali, Richard G. Allen, and Clarence Robison. 2009. *Application of METRC to Determine Evapotranspiration for Southeastern and Southcentral Portions of Idaho Including the Eastern Snake Plain for 2006*. Kimberly Research and Extension Center: University of Idaho, January.

Huete, A. R. (1988). A Soil-Adjusted Vegetation Index (SAVI). *Remote Sensing of Environment*, 25:295-309.

Huete,A.R., H.Q.Liu, K.Batchily and W.vanLeeuwen, 1997. A comparison of vegetation indices over a Groval Set of TM Images for EOS-MODIS. *Remote Sensing of Environment*, 59:440-451.

Hunsaker, D.J., Pinter, Jr., P.J. and Cai, H. (2002) Alfalfa basal crop coefficients for FAO–56 procedures in the desert regions of the southwestern U.S. *Trans ASAE*. 45(6):1799–1815.

Hunsaker, D. J., Pinter, P. J., Jr., Barnes, E. M., and Kimball, B. A. (2003). "Estimating cotton evapotranspiration crop coefficients with a multispectral vegetation index." *Irrig. Sci.,* 22(2), 95–104.

Kustas, W. P., and Norman, J. M. (2000). "A two-source energy balance approach using directional radiometric temperature observations for sparse canopy covered surfaces". *Agronomy Journal*, 92(5), 847–854.

Mutziger, A.J., Burt, C.M., Howes, D.J. and Allen, R.G. 2005. Comparison of measured and FAO-56 modeled evaporation from bare soil. *J. Irrig. and Drain. Engrg*., 131(1):59-72.

Neale, C.M.U., Bausch, W.C., and Heerman., D. F. (1989). "Development of reflectance-based crop coefficients for corn." *Transactions of the ASAE*, 32(6):1891-1899.

Neale, C.M.U., H. Jayanthi and J.L.Wright. (2005). Irrigation water management using high resolution airborne remote sensing. *Irrigation and Drainage Systems*. 19:321-336.

Payero, J.O., Neale, C.M.U., and Wright, J.L. 2004. Comparison of eleven vegetation indices for estimating plant height of alfalfa and grass. *Applied Engineering in Agriculture, ASAE*. 20:3:385-393.

Roerink., G. J., Su, Z., & Menenti, M. (2000). "S-SEBI: A Simple Remote Sensing Algorithm to Estimate the Surface Energy Balance". *Phys. Chem. Earth (B)*, 25:2, 147-157.

Su, Z. (2002). "The Surface Energy Balance System (SEBS) for estimation of turbulent heat Fluxes". *Hydrology and Earth System Sciences*. 6 (1), 85-99

SYSTAT. 2007. *Statistics III*. SYSTAT for Windows 12. SYSTAT Software Inc. .

Tasumi, M., Allen, R. G., Trezza, R., and Wright, J. L. (2005a). "Satellite-based energy balance to assess within-population variance of crop coefficient curves", *J. Irrig. and Drain. Engrg, ASCE*, 131(1), 94-109.

Tasumi, M., Trezza, R., Allen, R. G., and Wright, J. L. (2005b). "Operational aspects of satellite-based energy balance models for irrigated crops in the semi-arid U.S". *Irrigation and Drainage Systems*. 19(3-4):355-376.

Tasumi,T., R.Trezza, R.G. Allen, and C.W. Robison. (2007). Summary of the METRIC-MODIS Applica-

tion for the Middle Rio Grande Valley of New Mexico for Year 2005. University of Idaho Research and Extension Center Report submitted to the US. Bureau of Reclamation and NASA. 28 p

Tasumi, M. and Allen, R. G. (2007). "Satellite-based ET mapping to assess variation in ET with timing of crop development. *Ag. Water Man.* 88(1-3):54-62.

Tasumi, M., R.Allen and R.Trezza. (2008). At-surface reflectance and albedo from satellite for operational calculation of land surface energy balance. *ASCE J. Hydrol. Engrg.* 13(2):51-63.

Tolk, J.A. and Howell, T.A. (2001). Measured and simulated evapotranspiration of grain sorghum with full and limited irrigation in three High Plains soils. *Trans. ASAE*, 44(6):1553–1558.

Vermote, E.F, N.Z. El Saleous and C.O. Justice. (2002). Atmospheric correction of MODIS data in the visible to middle infrared: first results. *Remote Sens. Environ.* 83(1-2):97-111.

Wright,J.L., (1982). New evapotranspiration crop coefficients. *Journal of Irrigation and Drainage* 108:57-74.

Wright,J.L., (1991). Using weighing lysimeters to developed evapotranspiration crop coefficients. Proceeding of the International Symposium on Lysimetry, Honolulu, Hawaii, ASAE.

Appendix A. ETrF Analysis for Year 2006

Clarence W. Robison, PE
Richard G. Allen, PE, PhD

Nov 2009

Methods and Materials

The image ET_rF and NDVI products from the Garcia et al (2009) application of METRIC to southern Idaho for 2006 were used in this analysis. Table 1 identifies the image dates and satellite platform. Additionally, Table 1 summarizes the accumulated precipitation for 3 days preceding the image date at selected locations within Path 40 south. Field points identified by Tasumi and Lorite in their sampling of ET_rF from 2000 and 2003 applications of METRIC served as the base sampling location dataset.

When developing ordinary least squares regression relationships of ET_rF (dependent variable) to other independent variables such as NDVI, there is a implicit assumption that the independent variables are measures without error. Therefore we required that the area surrounding the sampling location was uniform with regard to independent variables such as NDVI and that the sampled point was representative of points surrounding it that may have impacted the derivation of ET_rF via METRIC.

Assessing the uniformity of the independent index and ET_rF for the sampling location basically

Table 1. Image Date and Source of Image used in Path 40 South ETrF versus NDVI Relationships in 2006

Image Date	Source	Day of Year	Prior 3-day Precipitation			
			TWFI	RPTI	Shoshone	PICI
Apr 25, 2006	LS-7	115	0.41	0.56	0.54	0.63
May 3, 2006	LS-5	123	0.01	0.00	0.00	0.10
May 19, 2006	LS-5	139	0.00	0.02	0.00	0.00
Jun 20, 2006	LS-5	171	0.00	0.00	0.00	0.00
Jul 22, 2006	LS-5	203	0.00	0.00	0.00	0.00
Aug 7, 2006	LS-5	219	0.00	0.00	0.00	0.05
Aug 31, 2006	LS-7	243	0.00	0.00	0.00	0.00
Sep 8, 2006	LS-5	251	0.00	0.00	0.00	0.00
Sep 24, 2006	LS-5	267	0.05	0.08	0.06	0.01
Oct 10, 2006	LS-5	283	0.26	0.21	0.12*	0.44

TWFI: Twin Falls AgriMet Weather Station
RPTI: Rupert AgriMet Weather Station
Shoshone: NOAA Coop Station in Shoshone
PICI: Picabo AgriMet Weather Station
**The NOAA cooperator reported 0.63 inches of precipitation on October 10th.*

consisted of calculating the standard error of the index for the pixel associated with the sampling location and it's adjoining eight pixels. In the work with the 2006 Path 40 south dataset, the sampling points were contained in a ArcGIS point shape file. These points were buffered out by 55 meters creating a circular polygon 110 meters in diameter. This circular polygon covers the eight adjoining pixels centers provided the sampling location is not in a extreme corner of a pixel cell. The zonal statistics of NDVI and ET_rF for each of the circular polygons created from the sampling points were determined using the zonal statistics tool in ArcGIS. From the zonal statistics, the standard error was determined by the following equation.

$$StdErr = \frac{StdDev}{\sqrt{(PixelCount)}} \quad [4]$$

The following graphic shows the standard error of NDVI with respect to average NDVI for the sampling polygons created from the points. The graphic represents a sampling point dataset applied to a Path 39 2006 image. The second graphic shows the standard error versus the mean of ETrF for the sampling locations. To limit the sampling locations to points in uniform areas, we applied a threshold value to the standard error and discarded locations with standard errors above that threshold.

Steps:

1. Buffer point layer, creating sampling circles. The buffer distance will depend on the raster cell size. The objective is to create a circle for each point that will cover the eight adjoining pixel cell centers.
2. Calculate zonal statistics for each sample circle. Depending where the sampling point is located within a pixel, the zonal cell count will range from 8 to 10.
3. Using the zonal statistics, or by computing a uniformity measure from the zonal statistics; discard sampling circles (ie, points) that have poor uniformity.

The Tasumi and Lorite sampling locations were filtered to only include those locations where the standard error of NDVI and ET_rF of the nine pixels surrounding the location was less than 0.002 for both ET_rF and NDVI. This was to insure uniform surface and thermal characteristics for a point – basically eliminating those points adjacent to a field boundary. Additionally, any sampling location located in or next to a LandSat 7 SLC gap were discarded. This resulted in a set of 249 sampling locations for Path 40 south as shown in Figure 1.

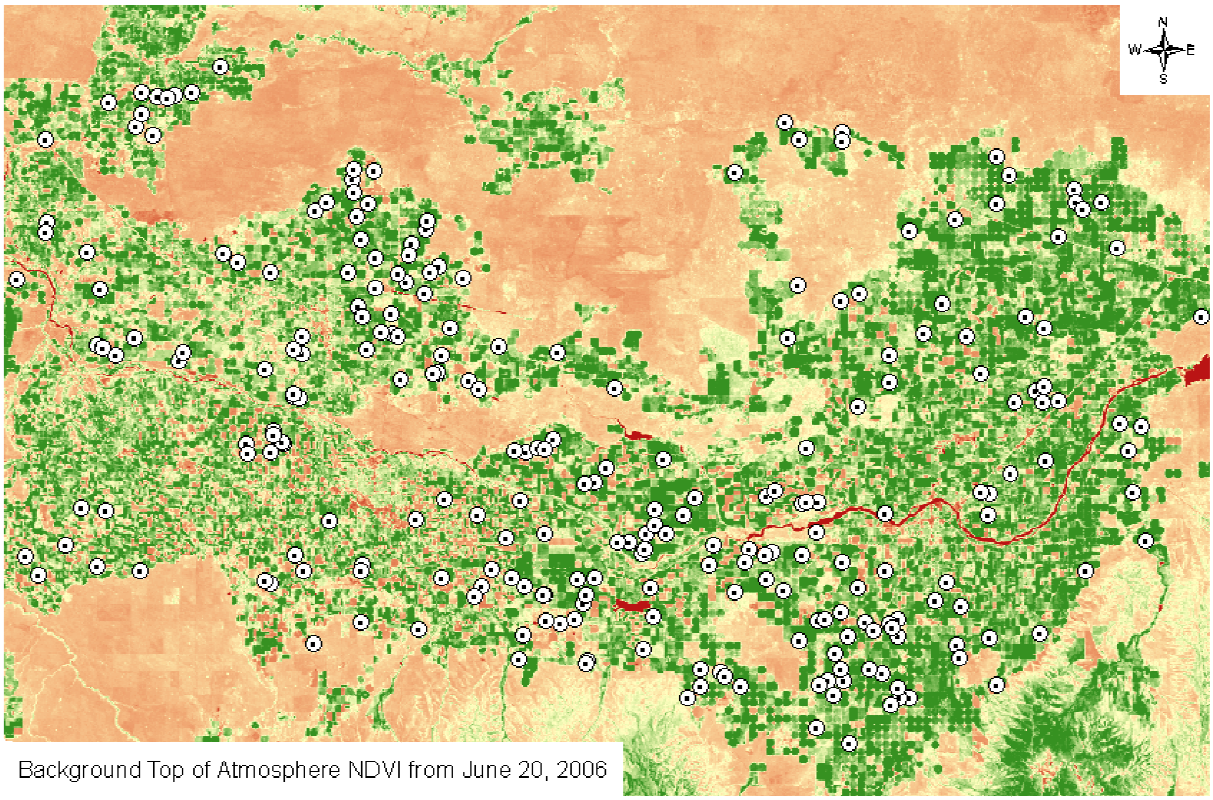

Figure 1. Sampling locations used in developing ET_rF versus NDVI relationship.

Using the 249 sampling locations, the 10 ET_rF and NDVI images were sampled using the ArcGIS Spatial Analyst Tool extract. The resulting datasets were imported into SYSTAT Statistical Analysis (SYSTAT 2007) software to determine linear relationships with ordinary least squares regression (OLS). The selected OLS relationships where then applied to selected fields within Path 40S. The fields select had areas between 30 and 300 acres in size with an effective area to perimeter ratio between 2 and 3.

Analysis

The first analysis looked at the relationship without regard to day of year (DOY) and preceding precipitation. The data points are shown in Figure 2 with the fitted regression line. The fitted regression line is:

[5]

with a R-square of 0.637. Examination of the scatter plot reveals the soil moisture evapotranspiration component for low NDVI values. This soil moisture evapotranspiration is not related to NDVI. However, in water allocation studies, pre-irrigation in the spring and irrigation for tillage operations in the fall should be accounted for. Referring back to Table 1, the first and last images followed a wet period for the western, eastern, and northern portion of the area. To explore the impact of antecedent rainfall on the ET_rF vs. NDVI relationships, a regression analysis was performed for each image date. Results are summarized in Table 2.

Table 2. OLS Results for each Image (249 sample points)

Image Date	04/25	05/03	05/19	06/20	07/22	08/07	08/31	09/08	09/24	10/10
Day of Year	115	123	139	171	203	219	243	251	267	283
Constant	0.45	0.08	0.24	-0.09	0.38	0.26	-0.01	0.07	0.21	0.45
95% Upper CL	0.48	0.11	0.29	-0.05	0.42	0.29	0.03	0.14	0.24	0.48
95% Lower CL	0.41	0.05	0.20	-0.13	0.34	0.22	-0.04	0.00	0.18	0.42
Slope	0.43	1.03	0.89	1.22	0.80	0.90	1.19	1.32	0.92	0.56
95% Upper CL	0.52	1.09	0.99	1.28	0.85	0.95	1.25	1.46	0.98	0.63
95% Lower CL	0.35	0.96	0.79	1.15	0.74	0.85	1.14	1.18	0.86	0.49
R-Square	0.29	0.90	0.57	0.83	0.76	0.84	0.89	0.58	0.77	0.50

The regression results suggest that that the regression coefficients are unique for each image date. However, because future years may not be similar to 2006 regarding timing and magntidutes of precipitation and irrigation events, individual relationships may not be appropriate for application to future or other image dates. Therefore, further analysis was conducted by combining images into seasonal groups and prior precipitation amounts.

From Table 2 and Figure 3, the early and late season relationships are similar with relatively high offsets and lower slopes than the mid season relationships. This is probably due to general significant precipitation over the area for the preceding three days in spring and fall. This would indicate that one should group the April and October images together and lump the remainder into a dry group. Within the "dry" group, there could be several groups. As shown in Figure 3, the July and August relationships contain a majority of points around an ET_rF of around 1 and a NDVI between 0.8 and 0.9, since it is the midseason period.

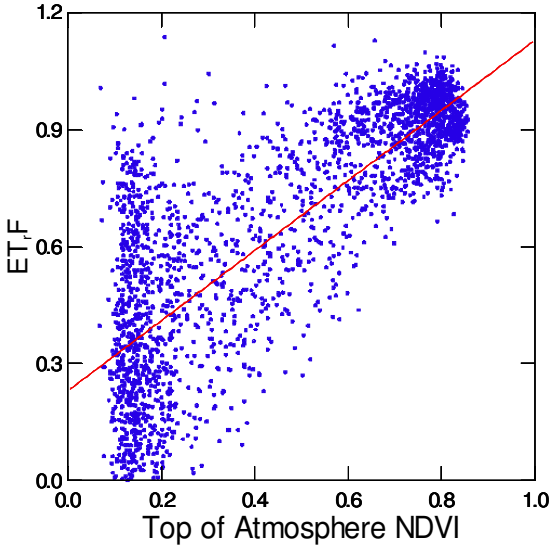

Figure 2. Scatter plot of ETrF versus NDVI for 2006 (LandSat Path 40S).

Table 3. Scatter Coefficients of ETrF versus Top of Atmosphere NDVI for each image.

Grouping	DOY	Constant (95%CR)	Slope (95% CR)	R-Square
All Images	115 – 283	0.231 (0.217-0.246)	0.897 (0.870-0.923)	0.637
Mid Season/Dry	123 – 267	0.141 (0.125-0.158)	1.034 (1.005-1.062)	0.718
Early/Late/Wet	115 and 283	0.449 (0.425-0.473)	0.502 (0.446-0.558)	0.385

Table 3 summarizes the coefficients for various grouping of the individual images. The values in parenthesis give the 95% confidence limits of the equation coefficients.

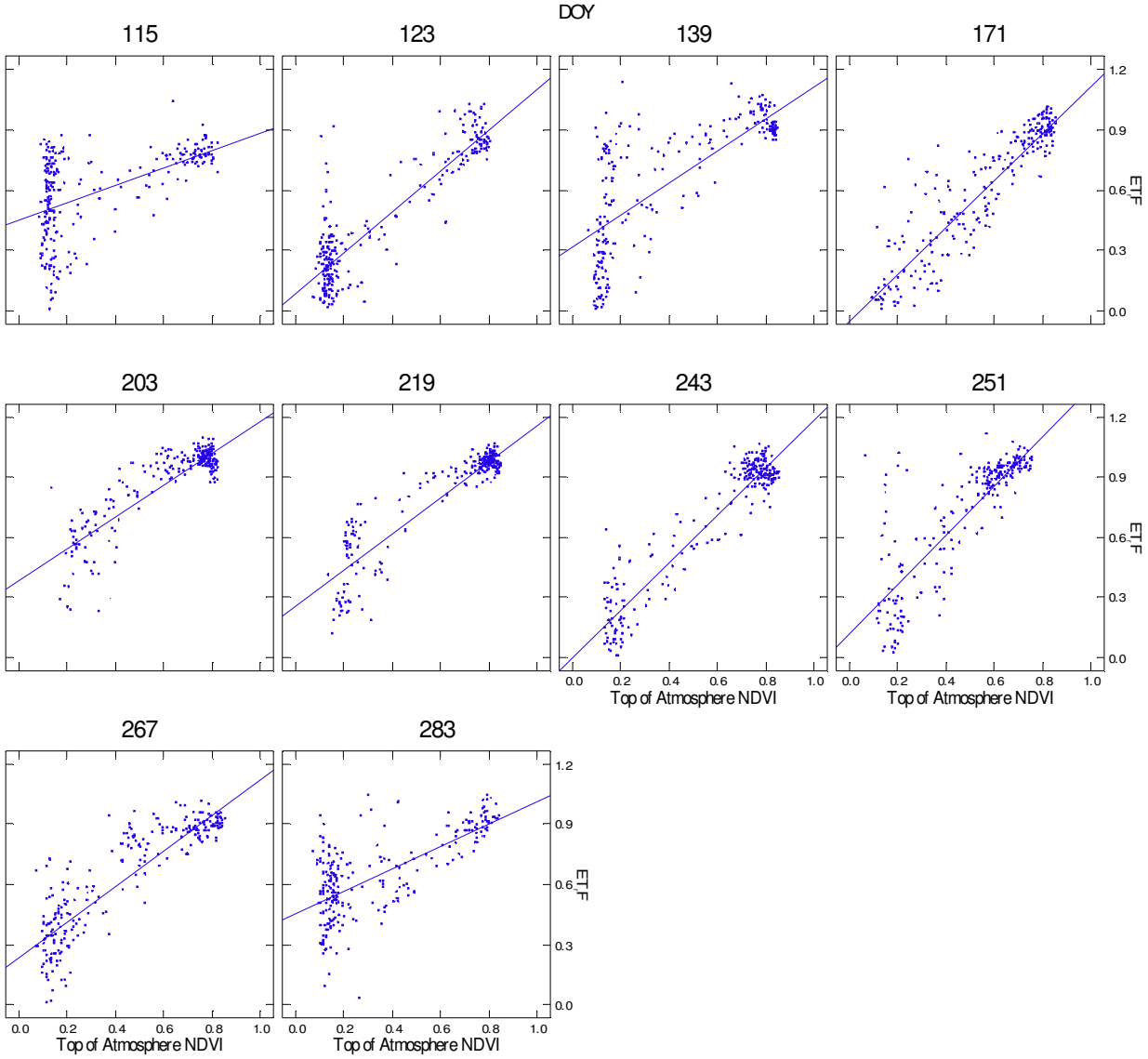

To examine potential interactions with vegetation type (crop), a preliminary crop classification was performed to determine the vegetation type of the 249 sampling locations for 2006. For the 249 sampling locations, the classification resulted in identifying 28 as alfalfa, 11 as beans, 33 as corn, 13 as potatoes, 16 as sugar beets, 16 as grain, 9 as winter grain, one as double crop, one as

Figure 4. ETrF – NDVI Relationships and Apparent Crop Type.

pasture, and 122 locations could not be reliably classified. Figure 4 visually shows the relationships described in Table 3. For the most of the crop classifications, the mid season/dry relationship captures the peak ET_rF cluster at high NDVI values with the exception of corn. The early/late/wet relationship appears to better estimate ET_rF at low values of NDVI where wet soil potential influences ET_rF from METRIC.

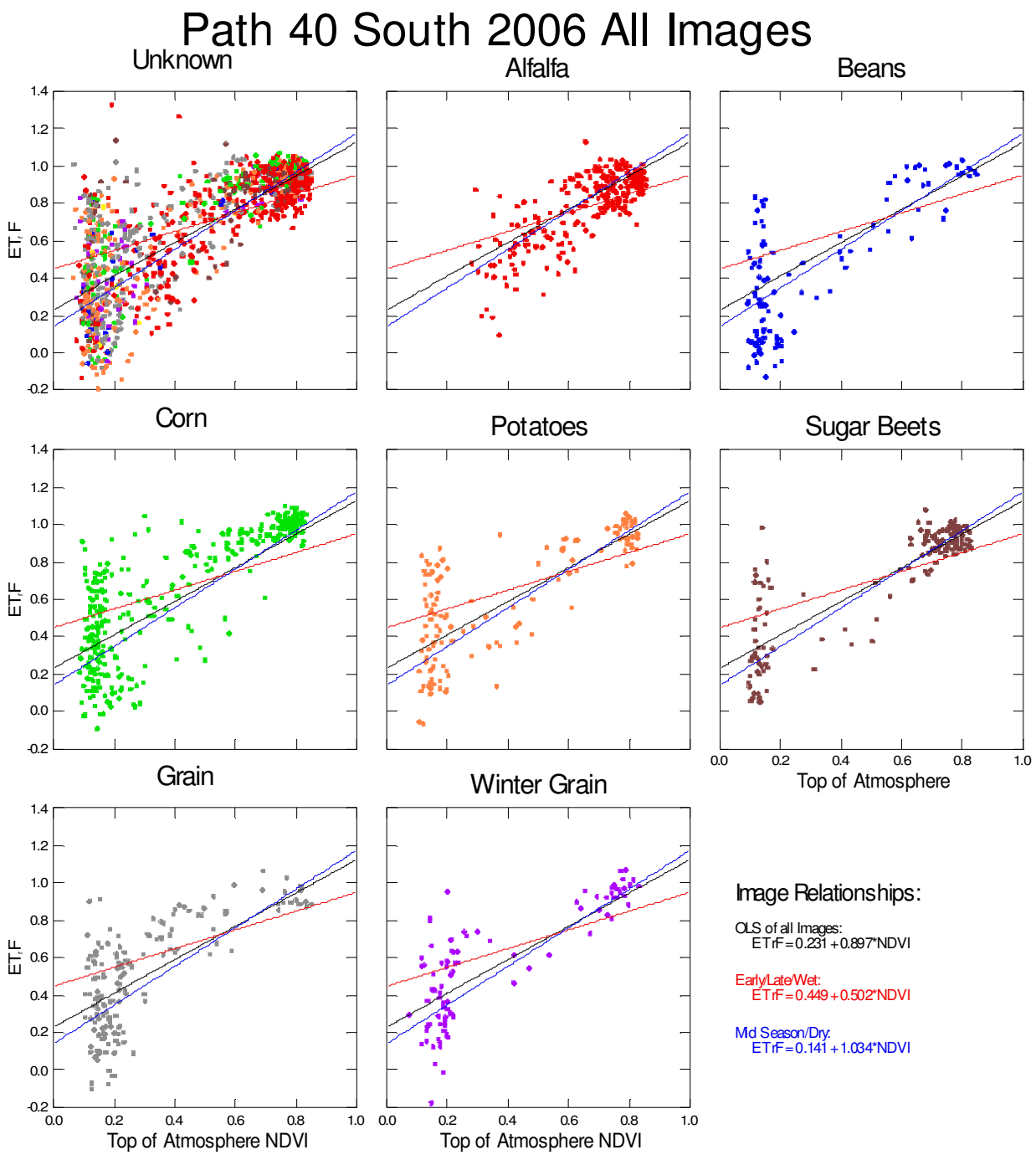

Test of ETrF – NDVI Relationships

The ET_rF – NDVI relationships listed in Table 3 were applied to selected certified land units (fields) within Path 40 South. The fields were selected based area and apparent shape. Additionally, fields overlaying any of the gaps from SLC failure associated with LandSat 7 images (Apr 25th and Aug 31st) were eliminated from the test of the relationship. Figure 5 attempts to show the location of these test fields.

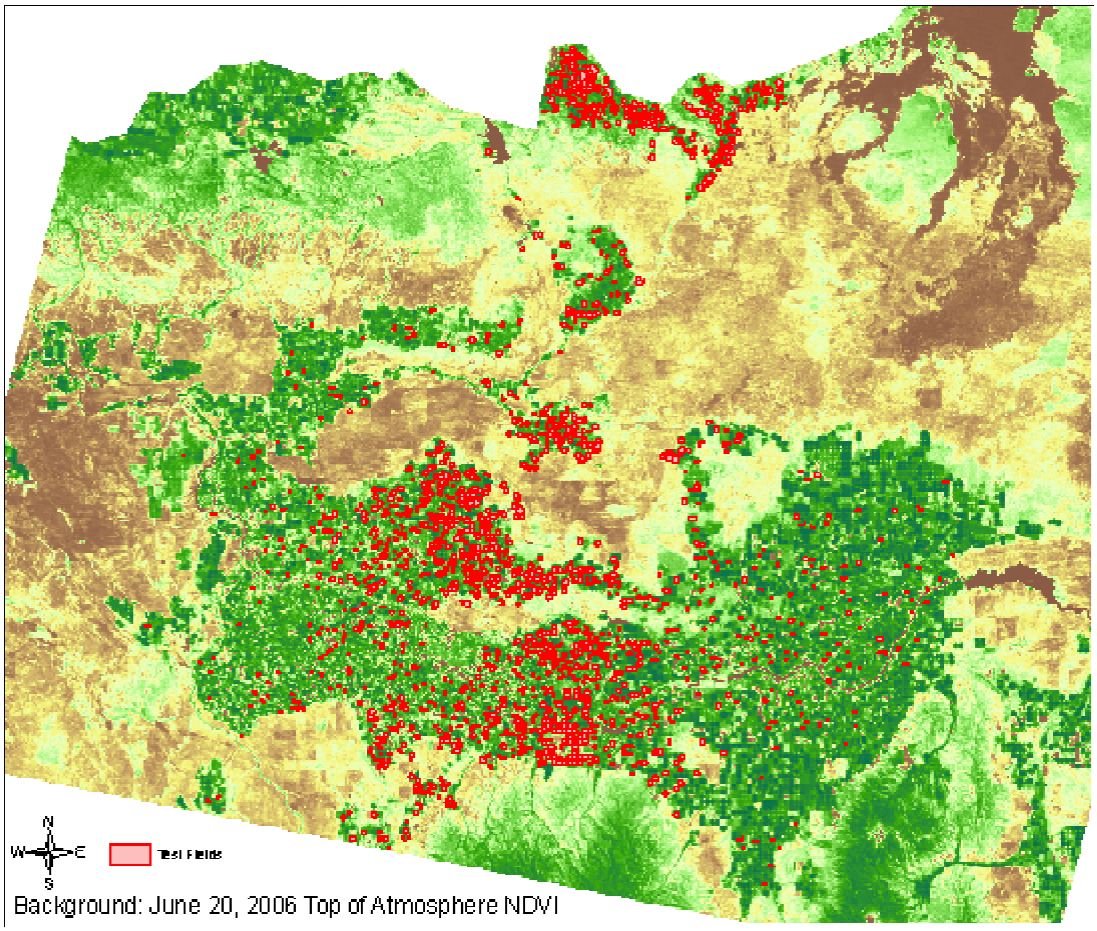

Figure 5. Location of test fields

The difference between the field mean estimated ET_rF from top of atmosphere NDVI and the field mean ET_rF from METRIC are summarized in Table 4. Overall, the average field mean difference of the 1761 test fields was 0.013. For test fields with in Minidoka county the estimated ET_rF was lower than that from METRIC by 0.021 on average. The estimated ET_rF for test fields within Twin Falls county was higher than that from METRIC by 0.031 on average.

Table 4. Difference (error) between Estimated ET_rF from Top of Atmosphere NDVI and ET_rF from METRIC for all 2006 images by county.

	All Locations	Blaine	Cassia	Gooding	Jerome	Lincoln	Minidoka	Twin Falls
Minimum	-1.28	-1.28	-0.602	-0.458	-0.535	-0.569	-1.060	-0.587
Maximum	0.704	0.704	0.494	0.576	0.432	0.507	0.564	0.551
Median	0.023	0.039	0.027	0.011	0.016	0.019	0.004	0.034
Arithmetic Mean	0.013	0.000	0.024	0.020	0.010	0.007	-0.021	0.031
95% Lower Confidence Limit	0.010	-0.009	0.010	0.009	0.007	0.001	-0.034	0.027
95% Upper Confidence Limit	0.015	0.009	0.037	0.030	0.013	0.014	-0.009	0.035
Standard Deviation	0.161	0.245	0.162	0.143	0.130	0.144	0.177	0.138

The results shown in Table 4 lead to an examination of the differences in the estimates with regard to ET_rF from METRIC. If the estimation equations are adequate, the differences should show no relationship to ET_rF from METRIC. This is not the case, it appears that the relationships are overestimating at low ET_rF values and underestimating at high ET_rF values.

Table 5. OLS Results for Crop Classification (75% confidence) for entire season.

Crop Classification	N (fields & days)	Constant	Slope	R-Square
Unknown	1220	0.246	0.876	0.61
Alfalfa	280	0.176	0.911	0.59
Beans	110	0.109	1.078	0.58
Corn	330	0.232	0.981	0.67
Potatoes	130	0.269	0.841	0.59
Sugar Beets	160	0.238	0.889	0.75
Grain	160	0.195	1.002	0.53
Winter Grain	90	0.209	0.966	0.65

Residuals have a significant trend in the south to north direction.

05/03/06 ETrF = 0.076 + 1.027*NDVI

Residuals have significant trends in the X(west-east) and Y(south-north) directions

Image Date	Source	Day of Year	TWFI	RPTI	Shoshone
Apr 25, 2006	LS-7	115	0.41	0.56	0.54
May 3, 2006	LS-5	123	0.01	0.00	0.00
May 19, 2006	LS-5	139	0.00	0.02	0.00
Jun 20, 2006	LS-5	171	0.00	0.00	0.00
Jul 22, 2006	LS-5	203	0.00	0.00	0.00
Aug 7, 2006	LS-5	219	0.00	0.00	0.00
Aug 31, 2006	LS-7	243	0.00	0.00	0.00
Sep 8, 2006	LS-5	251	0.00	0.00	0.00
Sep 24, 2006	LS-5	267	0.05	0.08	0.06
Oct 10, 2006	LS-5	283	0.26	0.21	0.12*

Appendix B. Applicability of Using Natural Neighbor Interpolation for NDVI

Clarence W. Robison, PE
Richard G. Allen, PE, PhD

May 2010

A procedure was tested to estimate and reconstruct field average NDVI from LandSat scenes impacted by the SLC failure of LandSat 7. The method uses the Natural Neighbor technique for filling in holes of missing data in images. The method yields approximate estimates for average NDVI for CLU's completely masked by SLC gap lines that have values representative of averages across the image. For CLU's that are partially masked by SLC gaps, the method raises NDVI values for low NDVI fields and lowers NDVI values for fields having high NDVI values due to introduction of biases from neighboring CLU's or from areas outside CLU's. The results were compared to a method that simply estimates a CLU average NDVI based on the residual of the CLU that is present (for partially masked CLU's) and that assigns a population wide NDVI value to those CLU's that are completely missing. We conclude that this latter method is equal or better in accuracy than using the Natural Neighbor approach, and that the additional resources required to fill partially masked fields using the Natural Neighbor method do not appear to be justified over this more simple method.

Methods:

Two NDVI images where used to test the procedures that were not impacted by the SLC failure of LandSat 7. One image was from June 20, 2006 in Path 40 Row 30 and the other image was from July 22, 2006. The NDVI images were 'broken' to represent the presence of SLC failure gaps by overlaying the images with a LandSat 7 image from Aug 31, 2006. NDVI from the broken images was sampled from 9250 fields based on a certified land unit shape file obtained from IDWR. The CLU's were limited to those fields having areas greater than 111,600 sq-meters (124 pixels representing approximately 27 acres) and less than 1,285,200 sq-meters (1428 pixels, approximately 320 acres). Additionally, the selected CLU fields were filtered on shape characteristics to eliminate sliver fields (narrow widths). Prior to breaking the two NDVI images, the images were sampled for average NDVI within each CLU to determine "true" NDVI for a field. The images were then broken, creating gaps in the NDVI image similar to those that would be in a LandSat 7 NDVI image, assigning "NoData" to pixels within a SLC gaps. The broken images were sampled using the same CLU field polygon coverage to determine average NDVI values for each field. The gaps in the broken images were filled using the Natural Neighbor interpolation algorithm in ArcGIS. The gap filled images were then sampled to determine CLU field average NDVI. The three estimates of NDVI were compared graphically to determine applicability of the natural neighbor method.

The *Natural Neighbor* interpolation method implement in ArcGIS is an interpolation method published by Sibson in 1981 and is known as "area-stealing" interpolation. It finds the closest subset of input samples to a query point and applies weights to them based on proportionate areas in order to interpolate. The natural neighbors of any point are those associated with neighboring Thiessen polygons.

Results:

The amount of a CLU field impacted by the SLC gap impacts the estimate of NDVI either by ignoring

the area in the gap or by filling in the gap with the natural neighbor interpolation technique. Figures 1 and 2 show the amount of error in the average NDVI estimate as a function of area remaining in a field after a gap is introduced. Figure 1 represents the end of June conditions with the end of July conditions shown in Figure 2. Both figures show that the Natural Neighbor interpolation of NDVI results in a closer estimation of average field NDVI (as compared to taking an average of the remaining pixels) as long as the field has 60% percent of its area outside of the gap. Below 50%, the estimated average field NDVI appears to be better estimated by just the field area remaining outside of the gap; unless, the gap entirely covers the field.

The natural neighbor interpolation method results in lower estimates of field average NDVI at high field averages of NDVI and higher estimates at low field average NDVI conditions as shown Figures 3 through 6. The last two figures (5 and 6) show the linear relationship between estimated NDVI and the original CLU NDVI. Linear regression of the original to the estimated CLU resulted in the following equations:

Period	Least Squares Regression	R^2	RMSE
Late June for the 7613 CLUs having at least one pixel missing due to SLC gap:			
	Original CLU NDVI = -0.012 + 1.029(Estimated NDVI Filled)	0.991	0.0178
	Original CLU NDVI = 0.002 + 0.998(Estimated NDVI Not Filled)	0.992	0.0183
Late July for the 7612 CLUs having at least one pixel missing due to gap:			
	Original CLU NDVI = -0.010 + 1.026(Estimated NDVI Filled)	0.990	0.0164
	Original CLU NDVI = 0.002 + 0.998(Estimated NDVI Not Filled)	0.994	0.0188

RMSE is the root mean square error. Units of RMSE are those for NDVI (dimensionless).

The RMSE of estimated field-average NDVI is shown in the following table as a function of amount of gap in the CLU. The error decreased as the amount of remaining field area increased. The RMSE was typically greater field-average NDVI was estimated from the natural neighbor filled images than when it was based on the average NDVI of the remaining CLU area, especially when large areas of the field lay within a SLC gap. When only small portions of fields lay within a SLC gap, the RMSE of the estimated NDVI from the natural neighbor filled image was marginally better.

Area Remaining after gapping	Percent of test fields	Field Count	Late June		Late July	
			RMSE using residual area	RMSE using NN Filling	RMSE using residual area	RMSE using NN Filling
0 – 10%	0.1%	12*	0.070*	0.137*	0.080	0.133
10 – 20%	0.6%	48	0.064	0.076	0.078	0.085
20 – 30%	1.4%	109	0.044	0.055	0.048	0.057
30 – 40%	3.2%	240	0.032	0.041	0.034	0.042
40 – 50%	4.8%	369	0.027	0.031	0.025	0.033
50 – 60%	8.4%	640	0.016	0.021	0.019	0.020
60 – 70%	16.0%	1222	0.016	0.015	0.015	0.015
70 – 80%	18.4%	1397	0.013	0.011	0.012	0.011
80 – 90%	25.0%	1900	0.009	0.008	0.009	0.008
90 – 99.99%	22.0%	1676	0.005	0.007	0.006	0.008

The asterisk indicates the totally masked out field was not included in the RMSE estimate. The field

count for the 0 – 10% classification in June was 11.

The late July test exhibits a higher spread in the differences between estimated CLU NDVI and the original especially with the natural neighbor interpolation method as shown in Figures 3 and 4.

Overlays of CLU units onto a gapped Landsat image are shown in Figures 7-9.

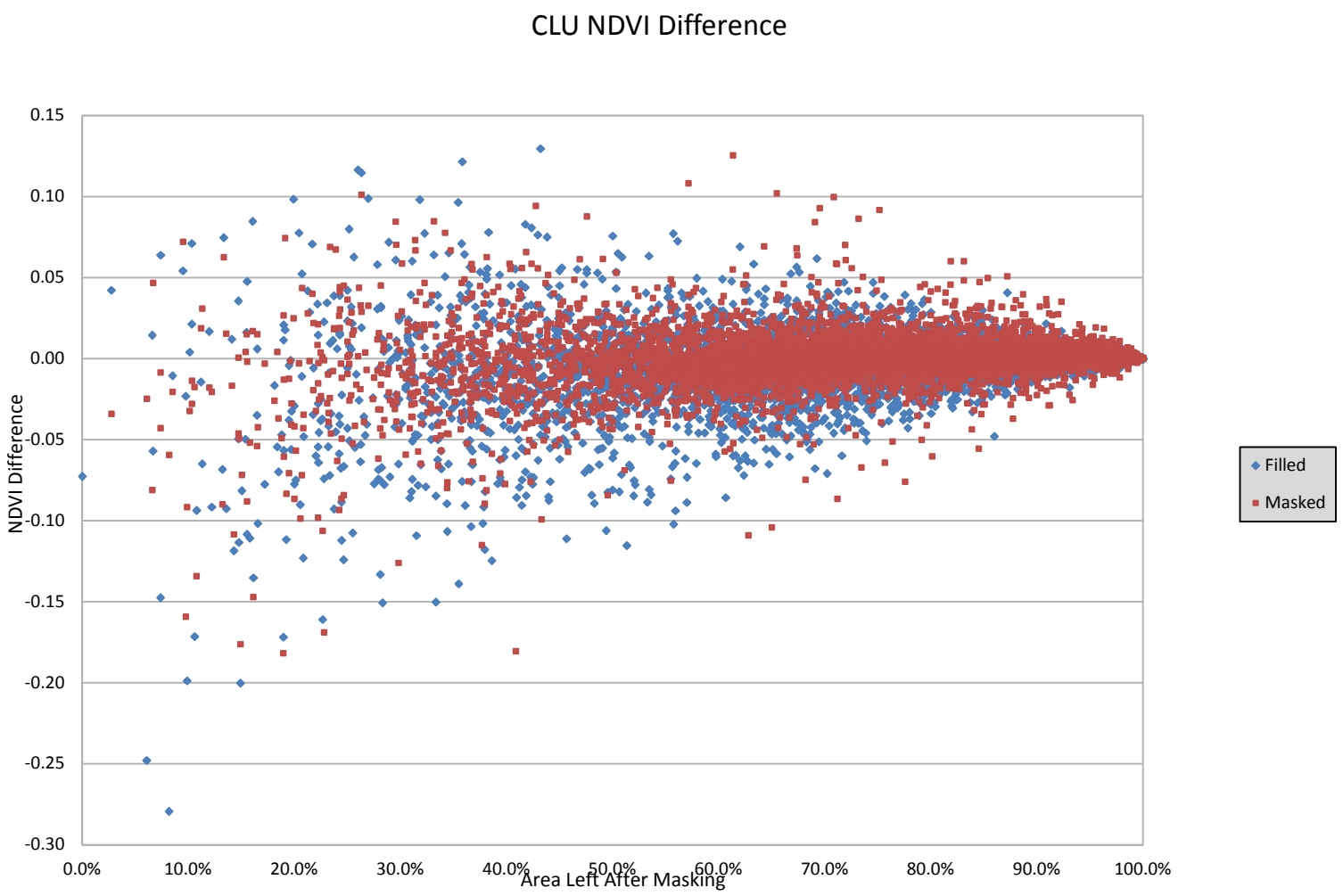

Figure 1. Difference in Estimated and Original CLU Average NDVI for late June as a function of gap area.

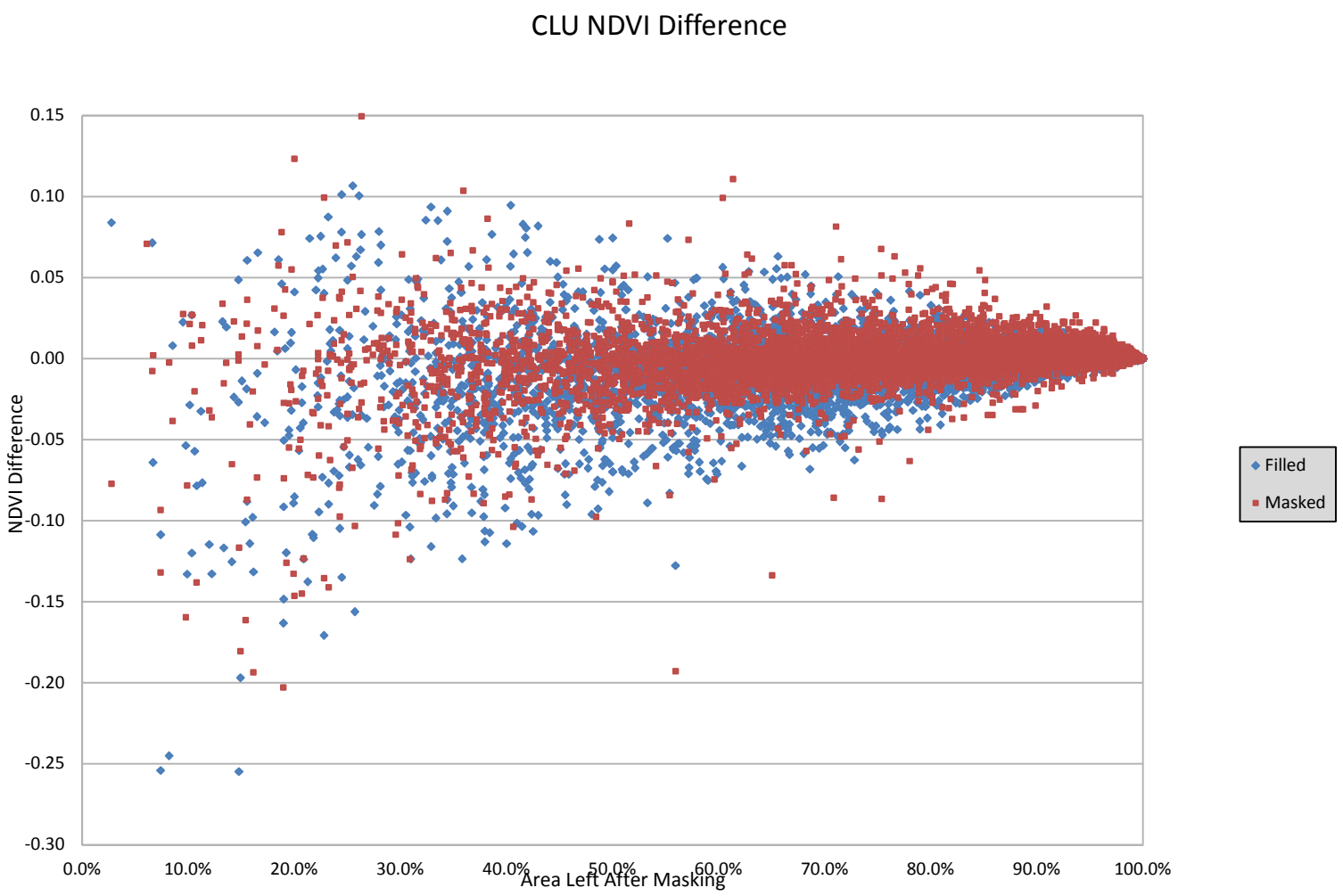

Figure 2. Difference in Estimate and Original CLU Average NDVI for late July as a function of gap area.

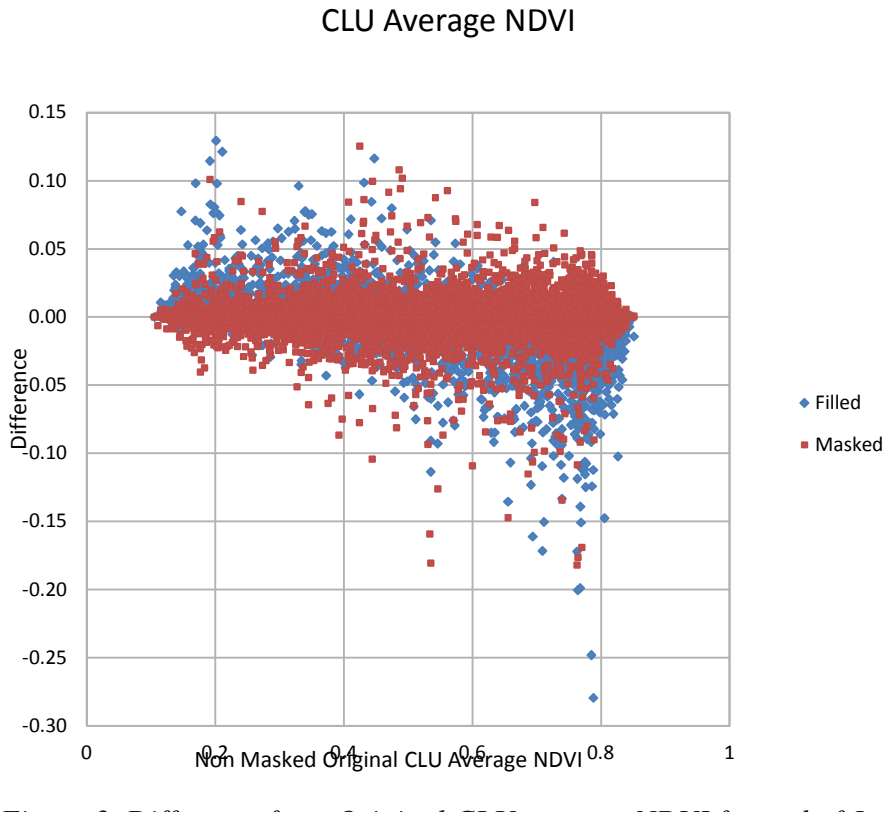

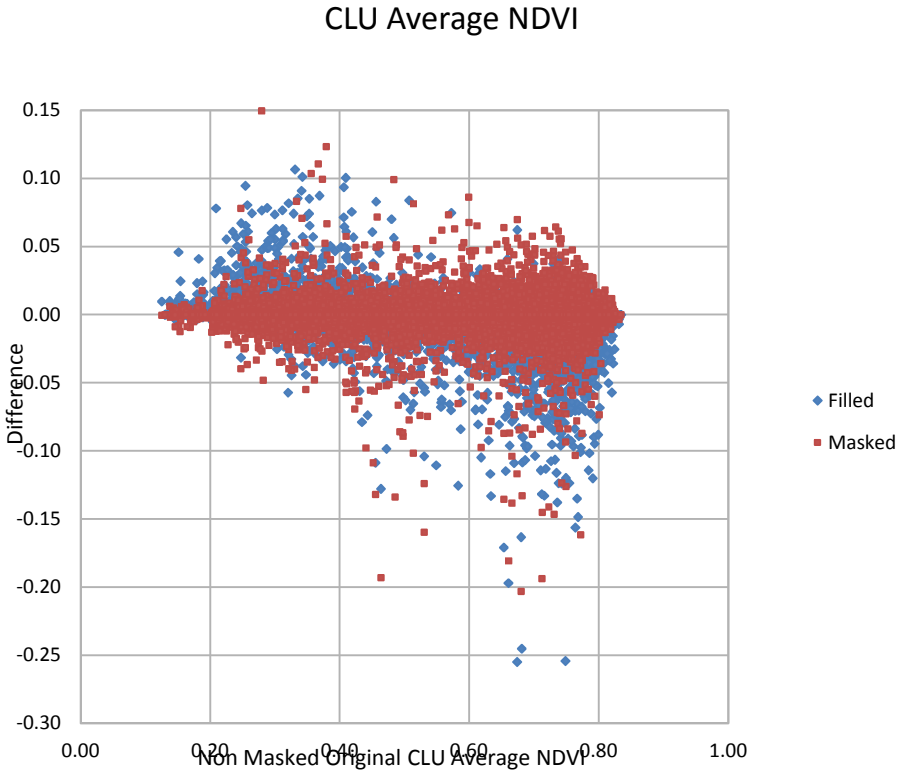

Figure 4. Difference from Original CLU average NDVI for end of July.

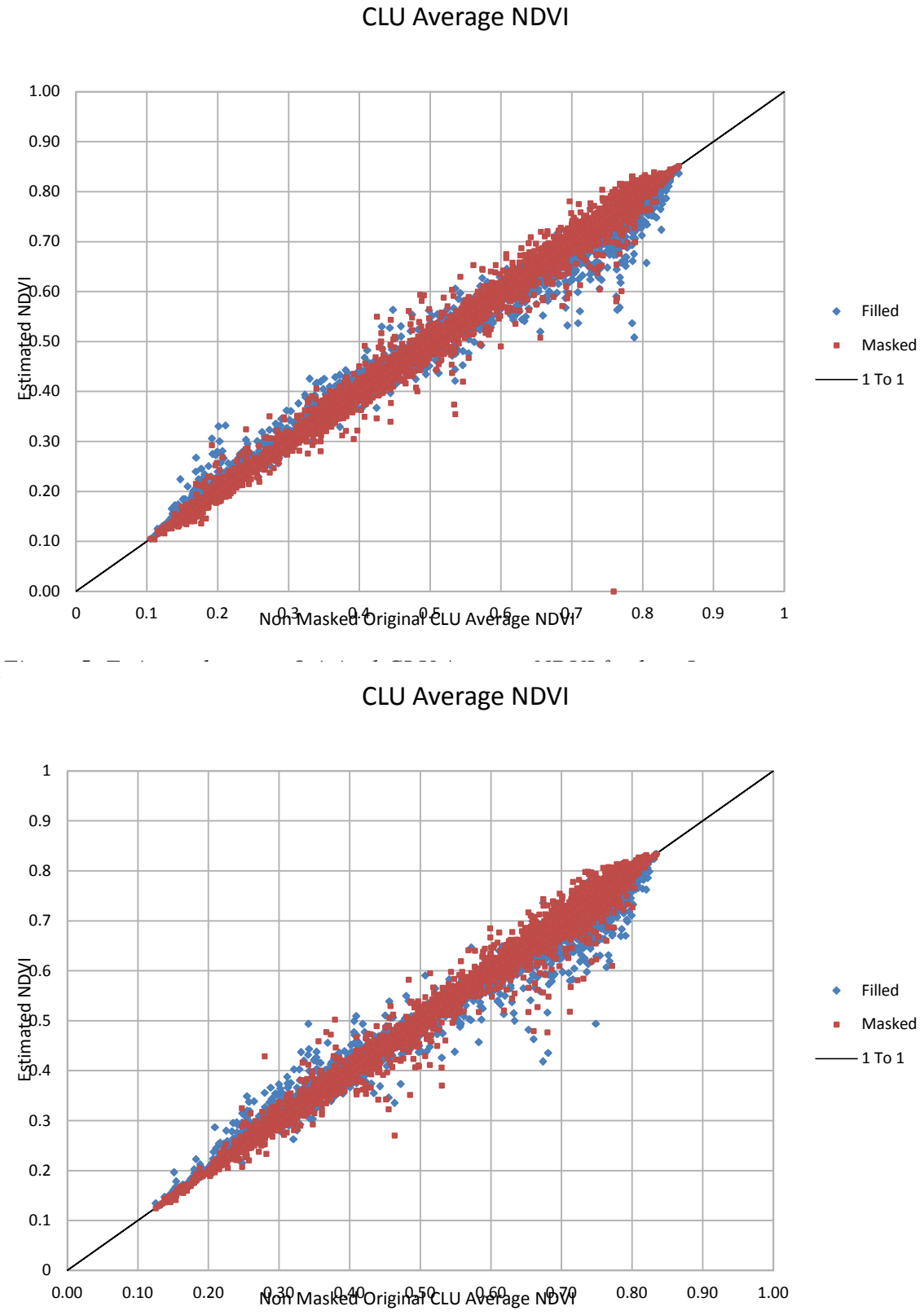

Figure 6. Estimated versus Original CLU Average NDVI for late July.

Suggested Procedure:

It is recommended that natural neighbor interpolation not be used to fill in gaps in Landsat 7 SLC-off images to determine CLU (field) average NDVI (for fields not entirely masked by the SLC gap), but rather base the CLU average NDVI on the average NDVI of remaining (present) pixels in the CLU. For the fields entirely masked by the SLC gap, there are two options: 1) assign an estimated average NDVI of all the CLU where a NDVI estimate is available, or 2) perform a natural neighbor interpolation on a buffered area of the CLU entirely masked. The CLU polygon would be buffered out until the polygon includes nonmasked areas on opposite sides.

The second option would require significantly more resources to perform and the resulting estimate of field average NDVI would still be a guess. The assumption is that vegetation of the totally masked CLU is similar to that of the nearest fields not totally masked.

Only one of the 9249 fields evaluated was completely masked out in the June image. None of the test fields were totally masked in the July images. Thus, only a very small percentage of fields (CLU's) are expected to be completely absent in an image.

The error (RMSE) in estimated NDVI for gapped images was less than 0.018 and 0.016 (in units of NDVI). This error may translate into approximately double this amount of error in crop coefficients (or ETrF) that are estimated from the NDVI (due to uncertainties in surface evaporation or water stress). This amount of error is within tolerance of what is typically regarded as uncertainty in traditional crop coefficient and ET estimates, which is 10 to 15%. The estimated uncertainty in METRIC ET estimates is considered to be 10% for individual fields.

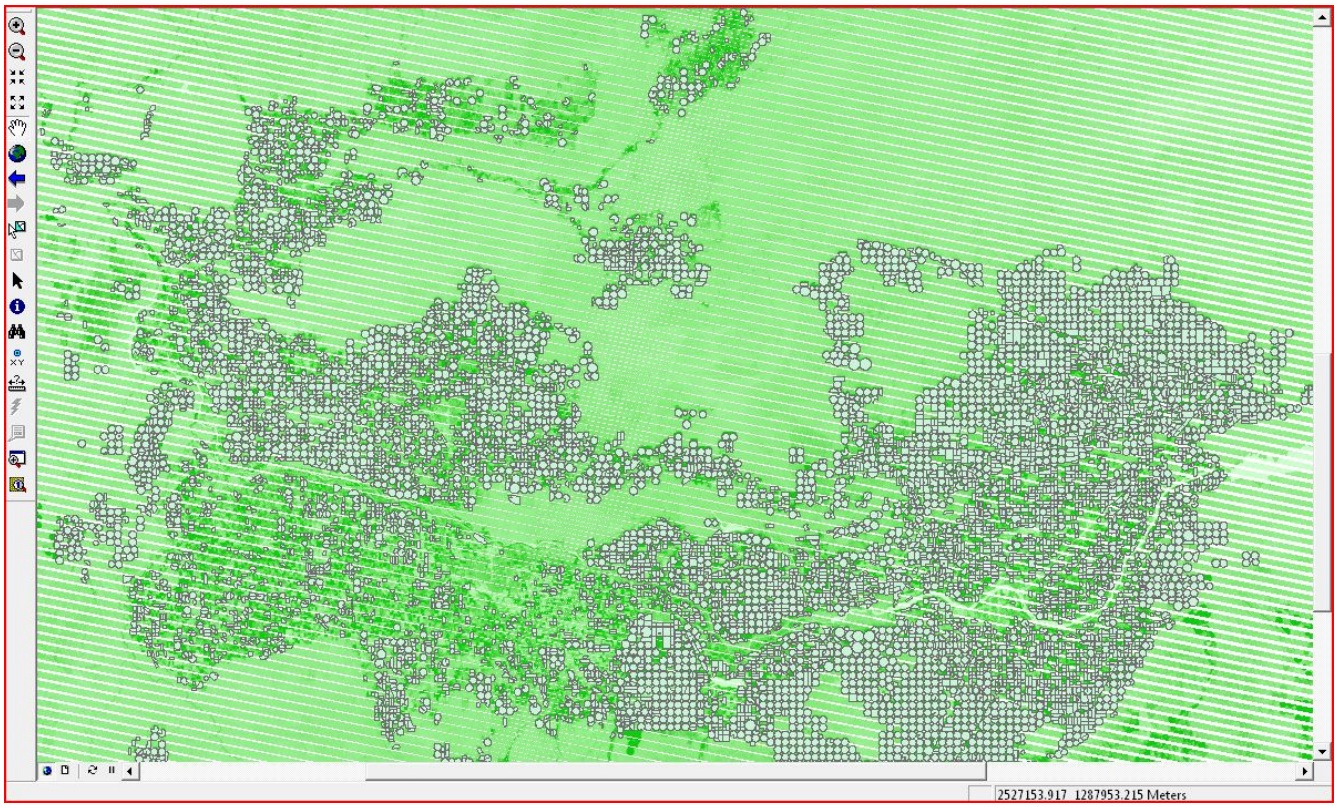

Figure 7. Field CLUs used in analysis overlaying artificially-created gaps in late June NDVI image.

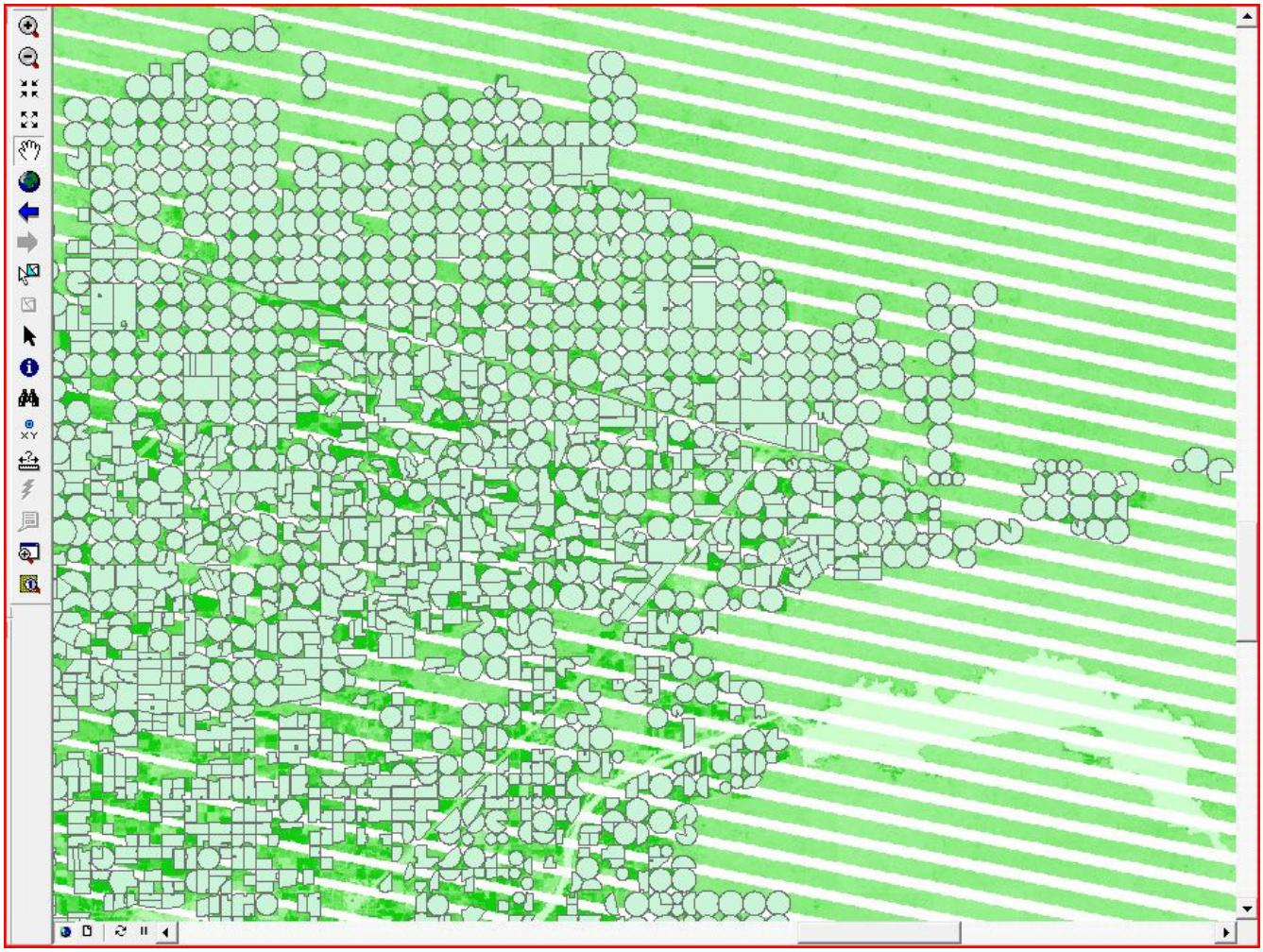

Figure 8 Closeup of Field CLUs overlaying late June 2006 NDVI on the east side of path 40 near Lake Walcott

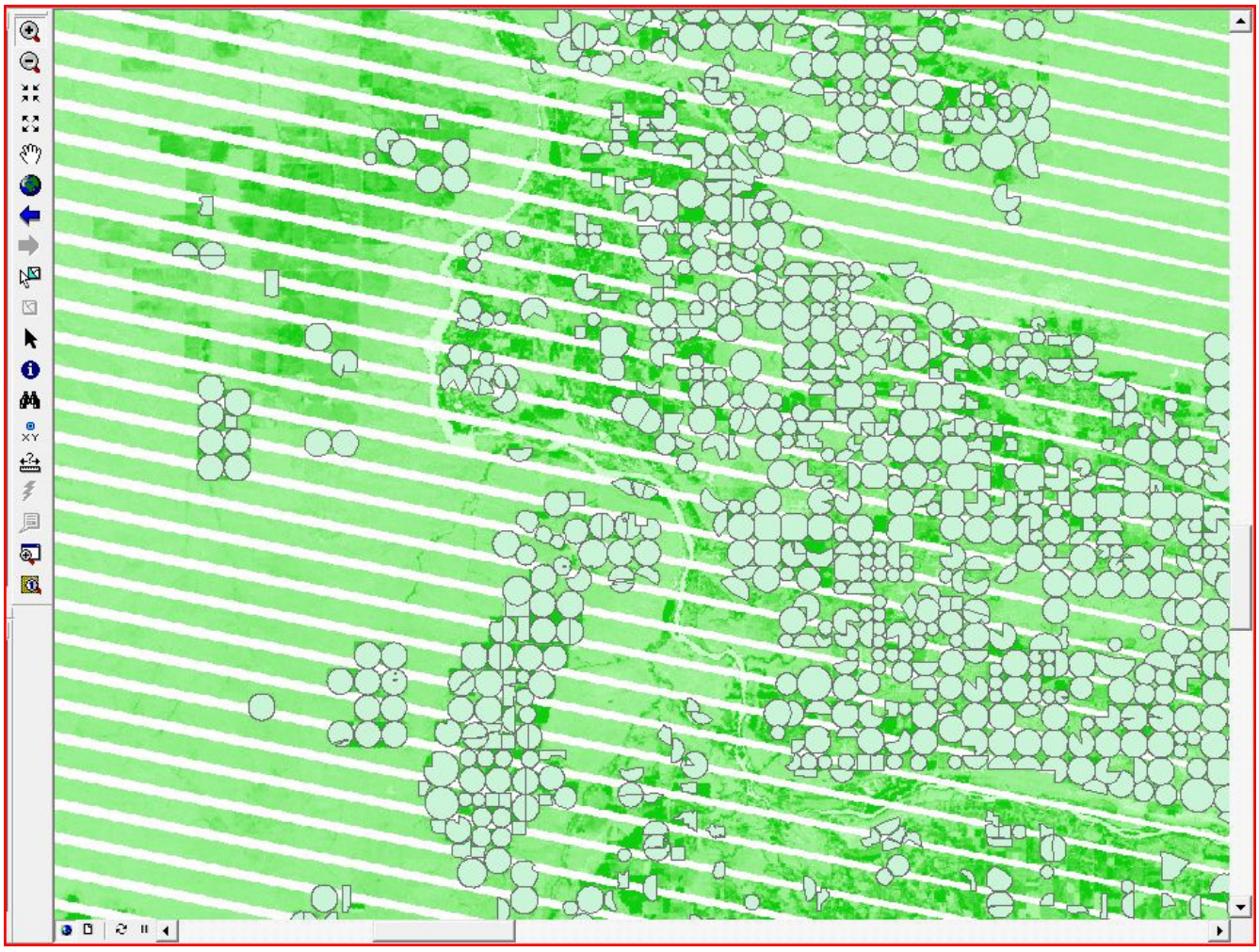

Figure 9 Closeup of Field CLU's overlaying late June 2006 NDVI on the western side of Path 40 in the Thousand Springs area.